

# High-Energy processes in astronomical sources

*Andrii Neronov*

University of Geneva

# Outline of the three lectures

## Lecture 1:

### Overview of high-energy sky

Thermal and non-thermal sources

Galactic and extragalactic sources

## Lecture 2:

### Particle acceleration / interaction / radiation mechanisms

Shock acceleration and acceleration by large scale electric fields

Synchrotron, inverse Compton, Bremsstrahlung emission by electrons / positrons

Pion production / decay emission from high-energy protons

## Lecture 3:

### Physics of high-energy sources (selected examples)

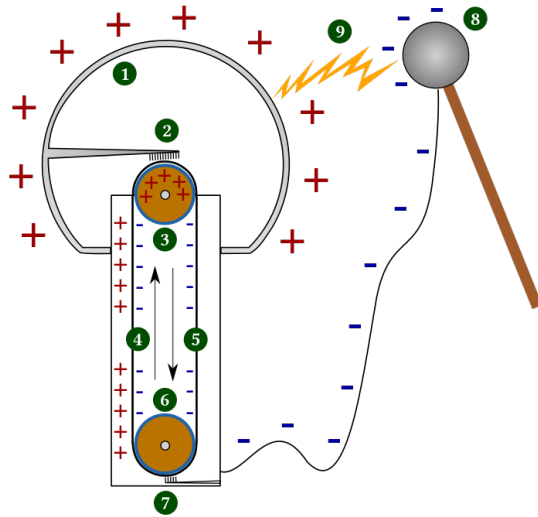
Pulsars / pulsar wind nebulae

Active galactic nuclei and blazars

The Galactic Center

# **Particle acceleration mechanisms**

# Particle acceleration in laboratory conditions

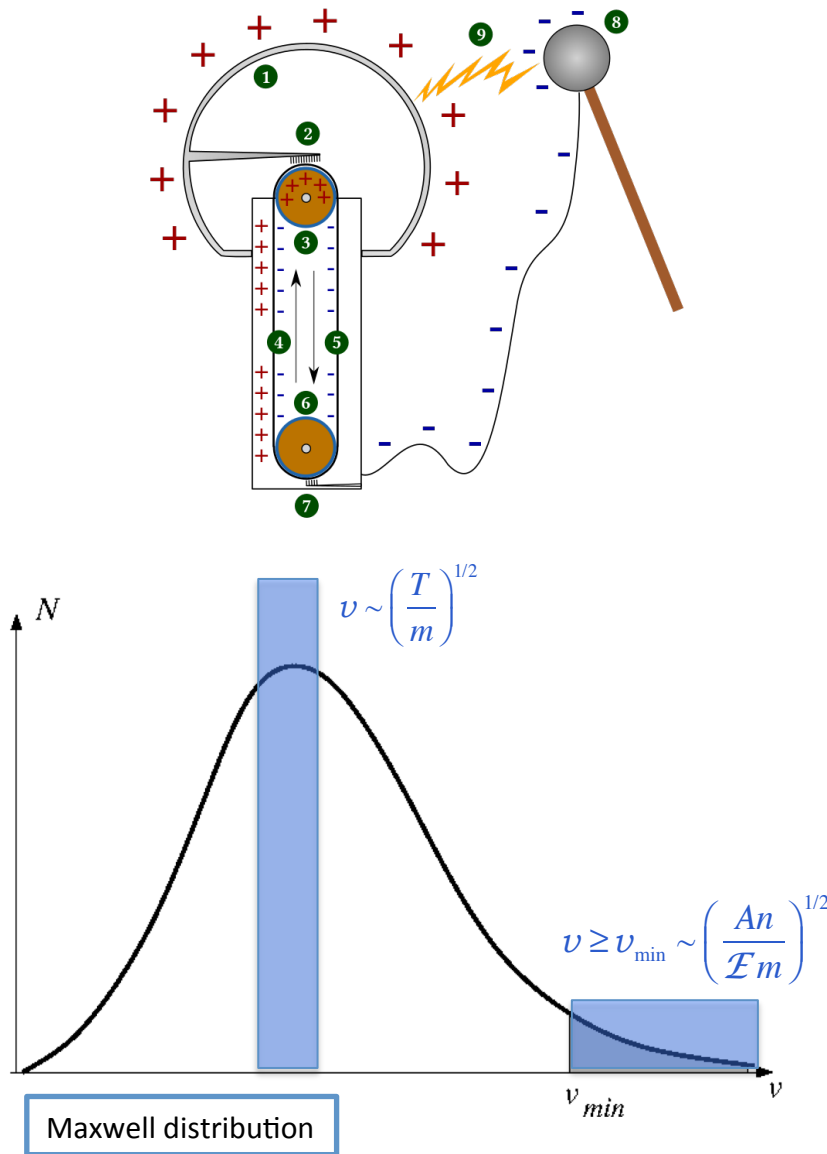


Particles are accelerated by electric fields  $E_{max} \sim qU$

First accelerator machines, Cockcroft-Wolton and Van de Graaf generators were “**linear accelerators**” creating a large voltage drop (up to MV), enough to boost electrons to relativistic energies.



# Particle acceleration in laboratory conditions



Particles are accelerated by electric fields  $E_{\max} \sim qU$

First accelerator machines, Cockroft-Wolton and Van de Graaf generators were “**linear accelerators**” creating a large voltage drop (up to MV), enough to boost electrons to relativistic energies.

Main limitation for particle acceleration was the **injection problem**: collisions of particles with ambient medium particles. The rate of momentum transfer in collisions is  $mvv_{\text{coll}}$ , where  $v_{\text{coll}}$  is the collision rate. For the acceleration to happen, this rate should be at least compensated the rate of momentum gain,

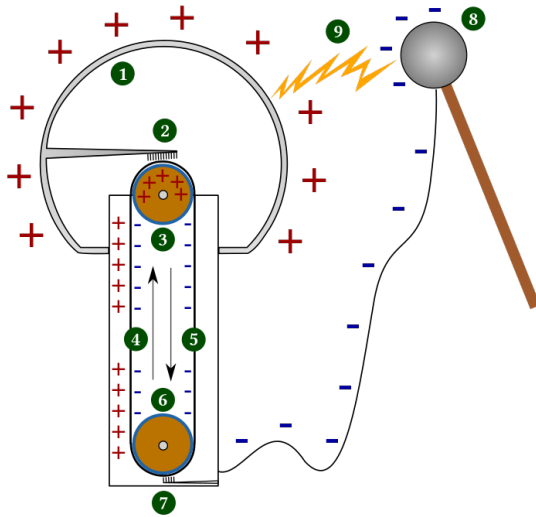
$$\frac{dp}{dt} = F = q\mathcal{E} \geq mvv_{\text{coll}}$$

The rate of collisions scales as  $v_{\text{coll}} \sim Anv^{-\kappa}$  ( $\kappa = 3$  for “Coulomb” collisions, i.e. deflections of particles by the Coulomb field of atomic nuclei). Only particles with

$$v \geq v_{\min} \sim \left(\frac{An}{\mathcal{E}m}\right)^{1/2}$$

could be accelerated. If the density of the medium  $n$  is high,  $v_{\min}$  is much larger than thermal velocity.

# Particle acceleration in laboratory conditions



Particles are accelerated by electric fields  $E_{max} \sim qU$

First accelerator machines, Cockroft-Wolton and Van de Graaf generators were “**linear accelerators**” creating a large voltage drop (up to MV), enough to boost electrons to relativistic energies.

Reduction of density of the medium relaxes the injection problem, but leads to the **discharge problem**

Particle energy gain over the distance  $\Delta x = v / v_{coll}$  in an accelerator of the size  $R$

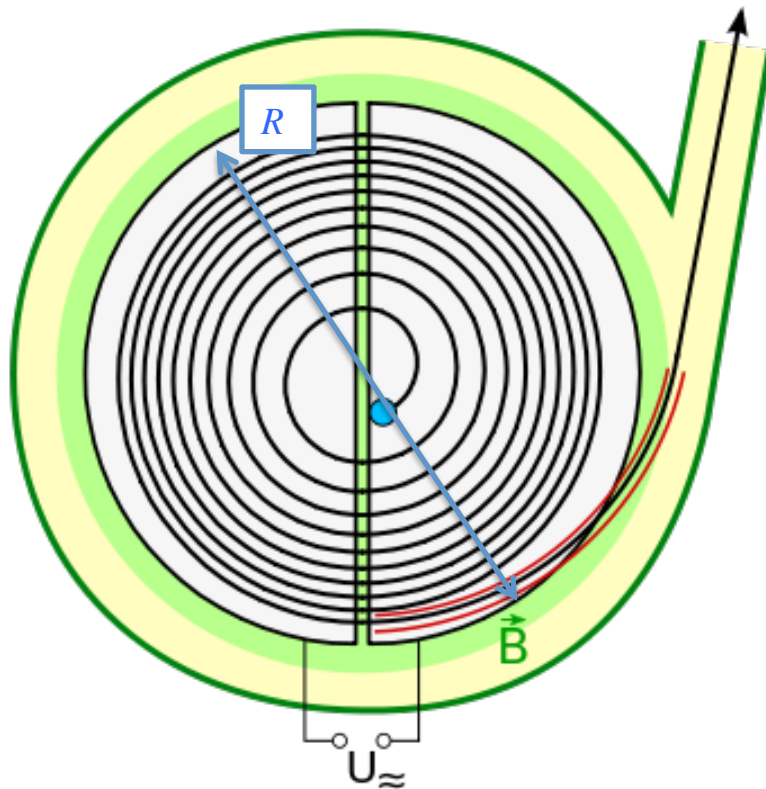
$$\Delta E \sim qU(\Delta x / R) \sim \frac{qUv}{Rv_{coll}} \sim \frac{qUv^4}{Rn}$$

If the density  $n$  is low enough,  $\Delta E$  is higher than ionisation energy of atoms. Ionised atoms and electrons are accelerated and also gain energy sufficient for ionisation. This leads to “cascade” ionisation and injection of large number charged particles.

Redistribution of charges in the acceleration volume erases external electric field as soon as

$$\frac{Q}{R^2} \sim \frac{en_e R^3}{R^2} \sim \mathcal{E}; \quad n_e \sim \frac{\mathcal{E}}{eR}$$

# Particle acceleration in laboratory conditions



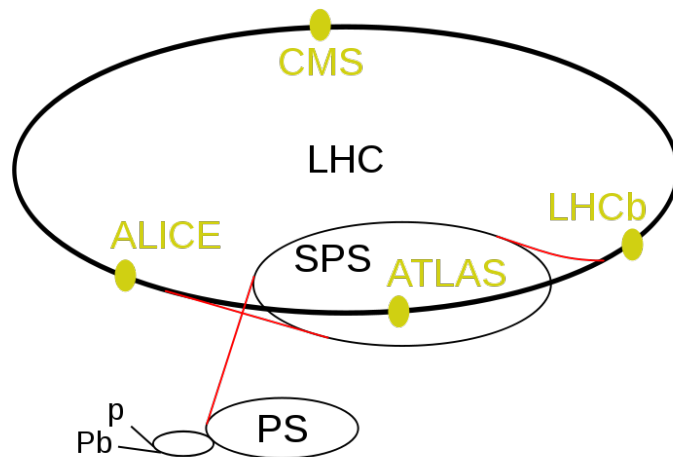
An alternative possibility is to accelerate particles in small voltage drops, but to systematically return the particle to the acceleration region. This is the principle of **cyclotrons / synchrotrons**.

Particles are accelerated in small steps  $\Delta E \sim q\Delta U$  and are systematically returned to the acceleration sites by magnetic field, along a circular trajectory

$$R_L = \frac{E}{eB}$$

Acceleration process could continue as long as

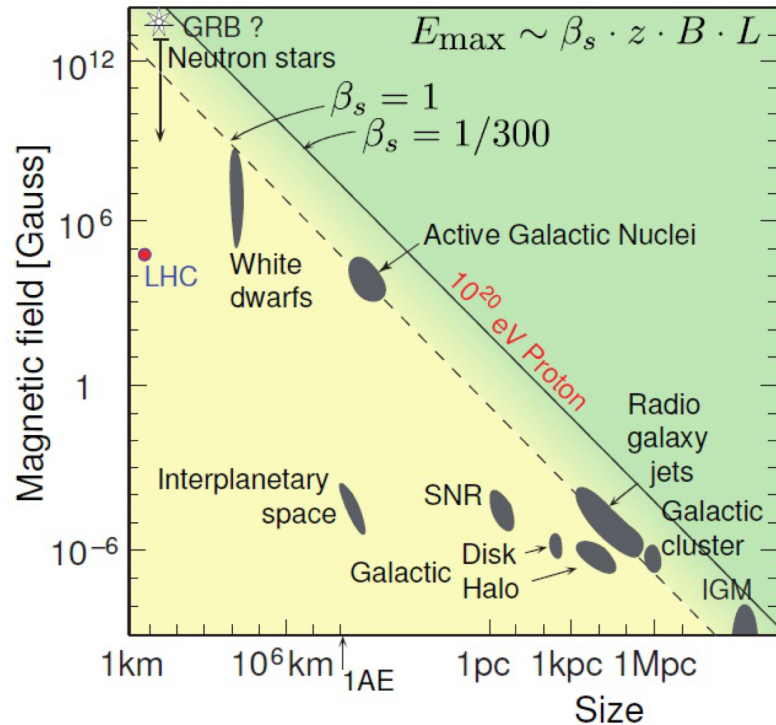
$$R_L < R; \quad E < E_{max} = eBR$$



Example: LHC

$$E_{max} \approx 3 \times 10^{13} \left[ \frac{B}{10^5 \text{ G}} \right] \left[ \frac{R}{10^6 \text{ cm}} \right] \text{ eV}$$

# Particle acceleration in astrophysical conditions



Physical conditions in astronomical sources are highly uncertain and are difficult to constrain observationally:

- we never measure electric fields
- we could get a limited knowledge of magnetic fields in astronomical sources.

In astrophysical conditions, particle acceleration process always operates in a medium of non-negligible density. This makes the “*injection problem*” ubiquitous.

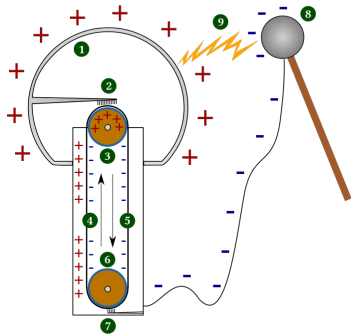
Astrophysical media are most often in an ionized state. Acceleration by large scale electric fields is only rarely possible because of “*discharge*” (charge redistribution erasing the accelerating electric field).

Maximal energies of particles are limited at least by the condition that particles should be retained in the accelerator by magnetic field

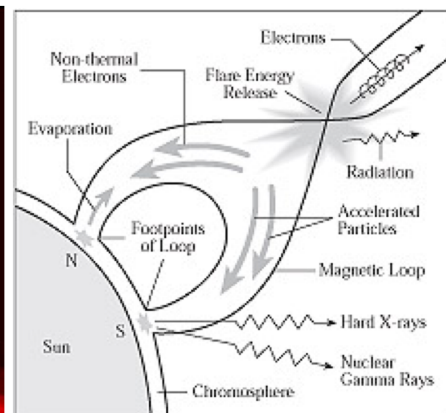
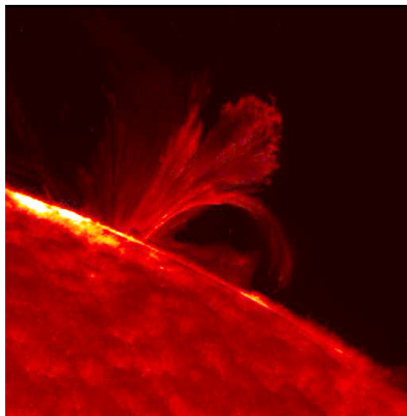
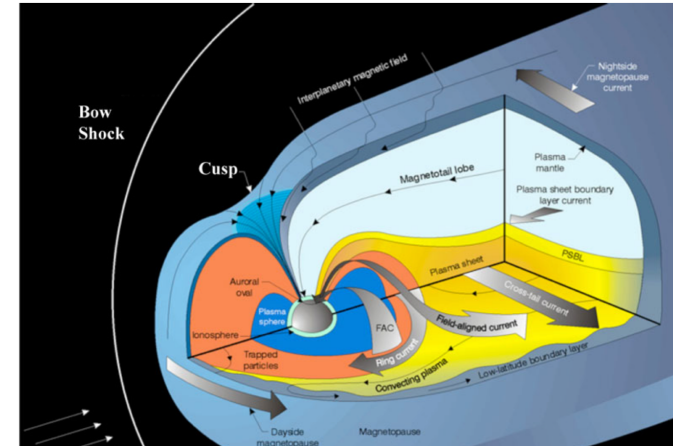
$$E_{\max} \simeq 3 \times 10^{13} \left[ \frac{B}{10^5 \text{ G}} \right] \left[ \frac{R}{10^6 \text{ cm}} \right] \text{ eV}$$

This restriction is represented via “Hillas plot”.

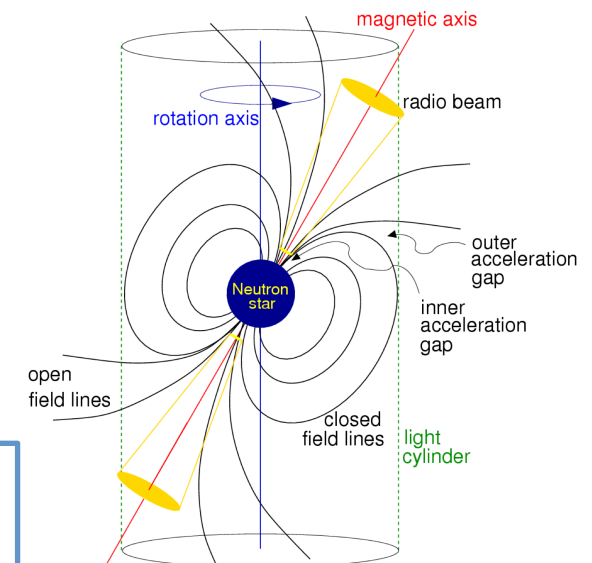
# Acceleration by large scale electric fields



Earth magnetosphere: large scale electric field is generated in the region of reconnection of magnetic field lines in the Earth's magnetotail.

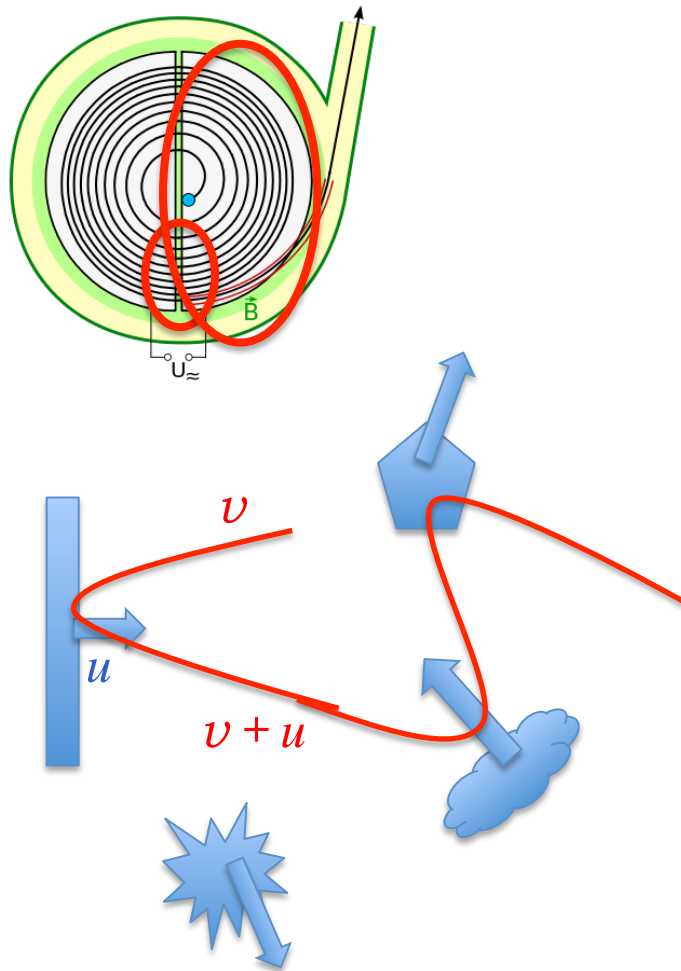


Solar flares: large scale electric field is generated in the region of reconnection of magnetic field lines.



Magnetospheres of pulsars: steady state large scale electric field is generated by rotation of magnetic field lines.

# Acceleration in small steps: Fermi process



In astronomical settings, abundant analogues of small acceleration steps are “kicks” with energy increase

$$\Delta E / E \sim v u$$

which particles get every time they bounce from a massive moving inhomogeneity of the medium (a cloud, a turbulent eddy etc).

Particles kept inside a source by magnetic fields could return systematically to one and the same or different inhomogeneities.

Particle acceleration rate is determined by the rate of particle-cloud collisions,  $\nu_{coll} = \sigma n v_{rel}$ , where  $v_{rel}$  is the relative velocity of particle and cloud.

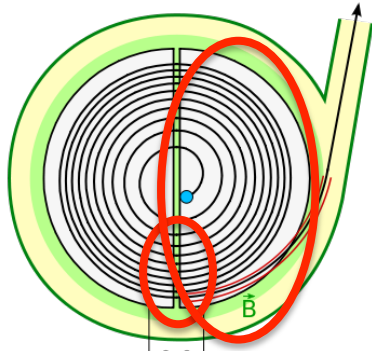
If the inhomogeneities move in random directions, there are head-on and tail-in collisions, which increase / decrease particle energy. Time average energy gain is

$$\frac{dE}{dt} \simeq E v u \sigma n [(v + u) - (v - u)] \simeq E \sigma n v u^2$$

proportional to  $u^2$ . This mechanism of acceleration is called “second-order Fermi acceleration”.



# Acceleration in small steps: Fermi process



In the second order Fermi acceleration energy gain is exponential in time:

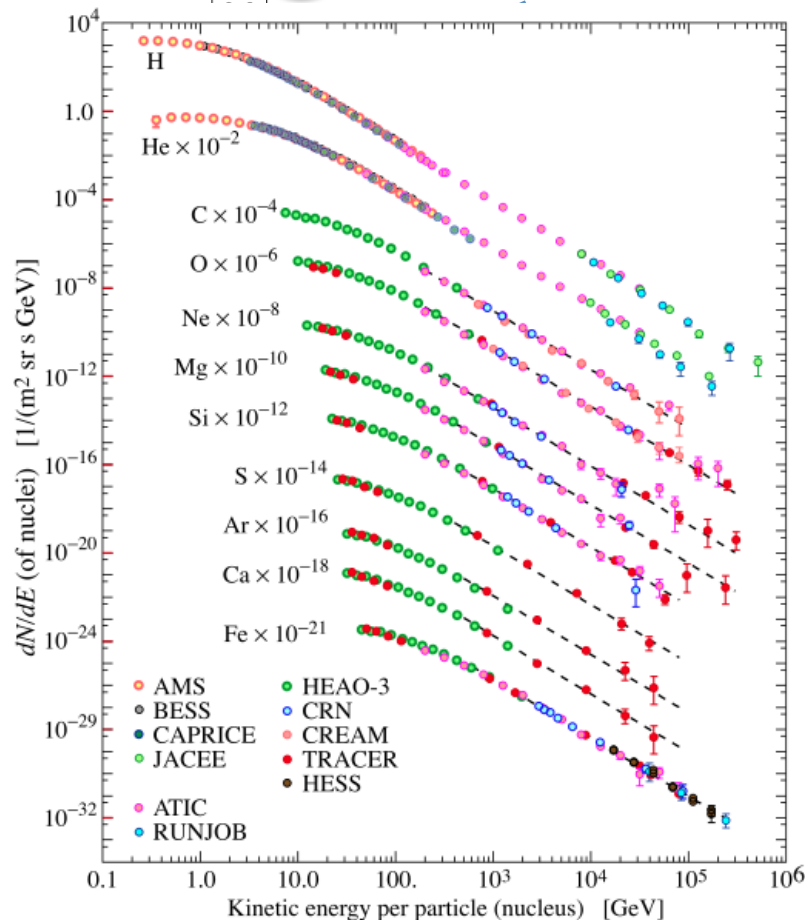
$$\frac{dE}{dt} \simeq E \sigma n v u^2; \quad E(t) \sim \exp(t / t_{acc})$$

$$t_{acc} = (\sigma n v u^2)^{-1}$$

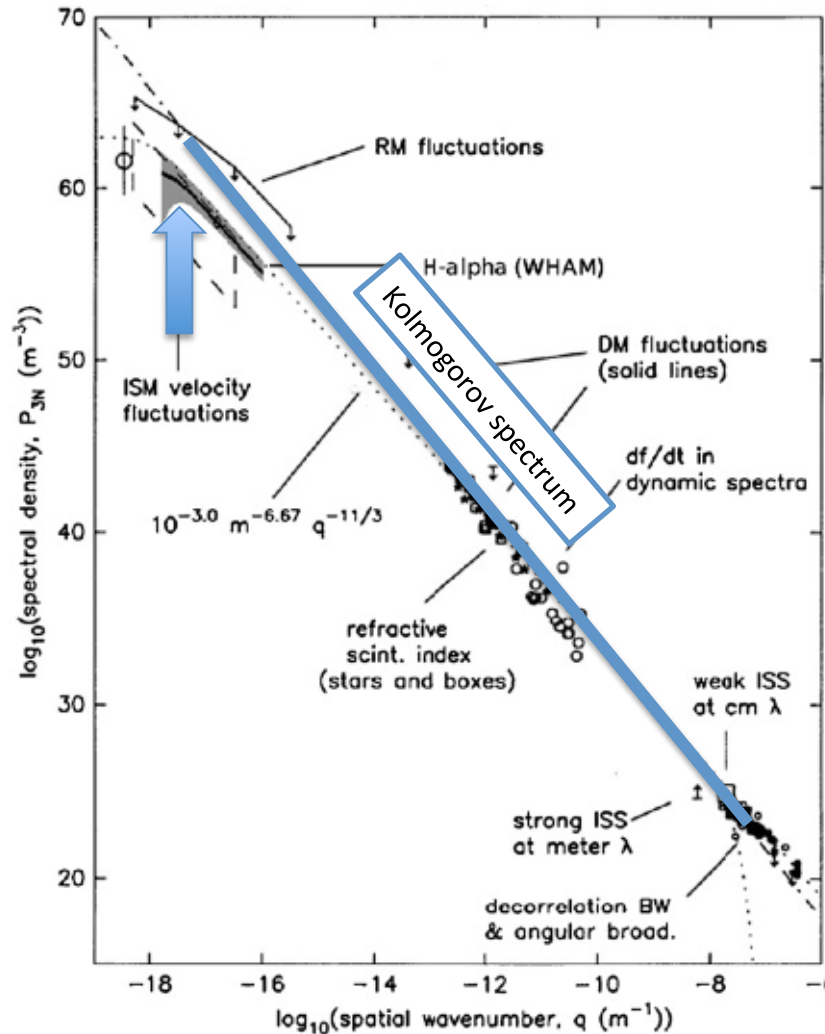
Most of particles residing in the acceleration volume for time  $t$  get approximately the same energy.

If particles are allowed to escape from the acceleration volume, with the escape time  $t_{esc}$ , the number of particles spending time  $t$  in acceleration volume decreases as  $N(t) \sim \exp(-t / t_{esc})$ .

Expressing  $t \sim t_{acc} \ln(E / E_0)$  one finds  $N(E) \sim E^{-t_{acc}/t_{esc}}$ .  
If acceleration and escape time are not functions of energy, the energy distribution of the accelerated particles is of powerlaw type.



# Example: Fermi process in the interstellar medium



Repeated supernova explosions deposit kinetic energy in the interstellar medium on the distance scale  $30\text{-}100\text{ pc}$ .

Magneto-hydrodynamic processes lead to development of turbulence and re-distribution of the energy initially injected in  $\lambda_{inj} \sim 30\text{-}100\text{ pc}$  scale to smaller distance scales (turbulent eddies).

Turbulence of the interstellar medium leads also to generation of turbulent magnetic field with energy density in equipartition with the mechanical energy density.

As a result, the interstellar medium is composed of randomly moving magnetized clumps of different size scales.

Charged particles bouncing from the magnetized clumps experience second-order particle acceleration.

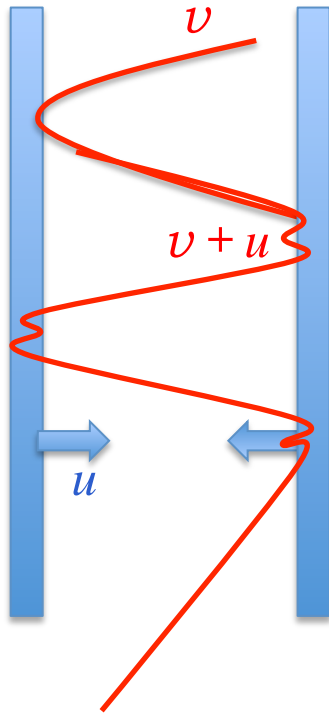
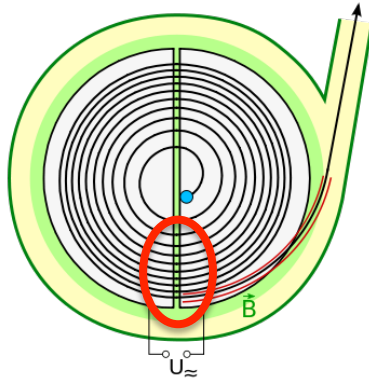
The acceleration time scale is

$$t_{acc} = (\sigma n v u^2)^{-1} \approx \frac{\lambda^3}{\lambda^2 u^2} \approx 10^{11} \left[ \frac{\lambda}{30\text{ pc}} \right] \left[ \frac{u}{10\text{ km/s}} \right]^{-2} \text{ yr}$$

.....



# Acceleration in small steps: shock acceleration



Similarly to the second-order Fermi acceleration, in shock acceleration particle energy is increased by the “kicks”  $\Delta E / E \sim vu$  which an accelerated particle gets when bouncing from a massive moving inhomogeneity of the medium (a cloud, a turbulent eddy etc).

Contrary to the second order Fermi process, energy is gained at each bounce. Particle energy grows exponentially with the time exponent  $t_{acc} \sim t_{bounce}$  in subsequent bounces until the particle escapes from the acceleration volume.

The number of particles residing in the acceleration volume during time  $t$  decreases exponentially  $N \sim \exp(t / t_{esc})$  with the time exponent  $t_{esc} \sim t_{bounce}$

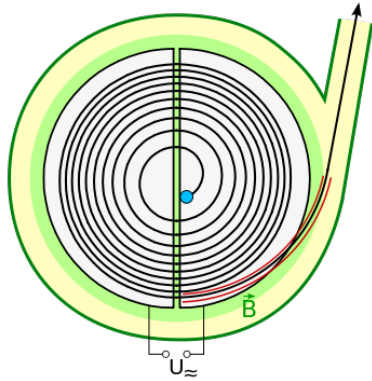
This leads to formation of a powerlaw-type spectrum

$$\frac{dN}{dE} \sim E^{-(1+t_{acc}/t_{esc})} \sim E^{-2}$$

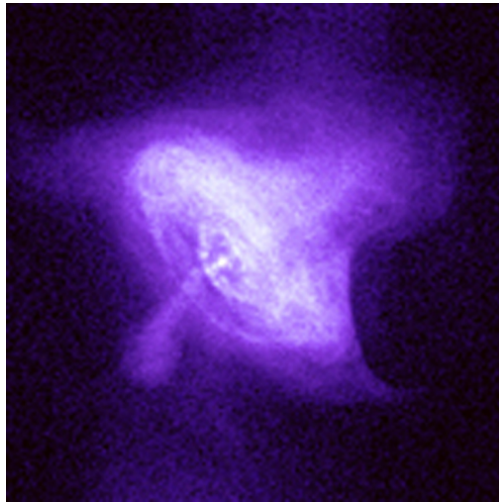
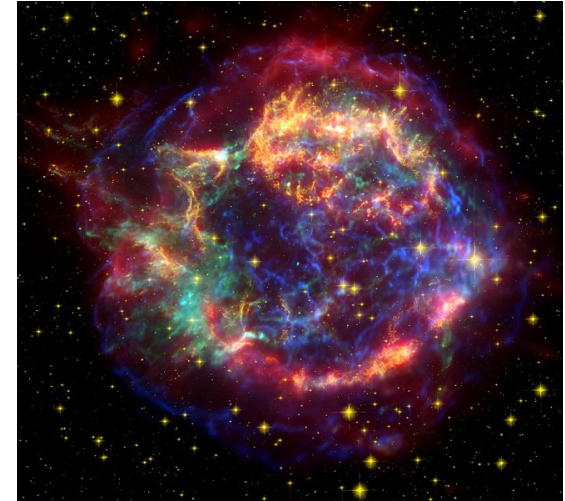
if  $t_{acc} \sim t_{esc}$ .

Maximal particle energies are limited by the condition that particle should be kept inside the shock by the magnetic field  $E_{max} = eBR$

# Acceleration in small steps: shock acceleration

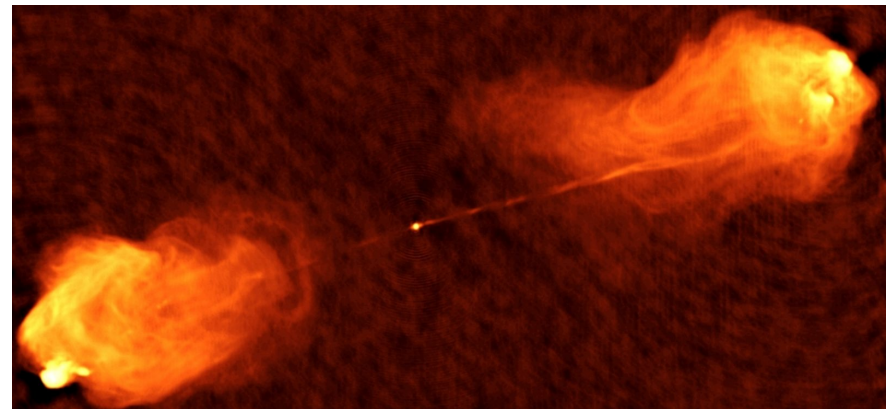


Supernova remnants: particles kept by the remnant magnetic field are bouncing inside the shock at the interface of ejecta with the interstellar medium.



Pulsar wind nebulae: particles kept inside the nebula by magnetic field are bouncing inside a shock at the interface of “pulsar wind” with the interstellar medium or supernova ejecta.

Radio loud AGN: particles kept inside the AGN jet or radio lobes are bouncing inside the shock at the interface between different portions of the jet or with the interstellar / intergalactic medium.



# Summary

**Particle acceleration mechanisms** could be divided onto fast, one-step acceleration by *large scale electric fields* and slow *multi-step acceleration* when particle is systematically returned to the acceleration region.

**Acceleration mechanisms** could operate only if the acceleration rate is high enough to overcome the *problem of injection*, both in laboratory and astrophysical conditions. This is facilitated if the density of the ambient medium is low.

**Acceleration mechanisms** could involving strong large scale electric fields could fail because of the *problem of discharge*: redistribution of charged particles in the acceleration volume compensates the external accelerating electric field.

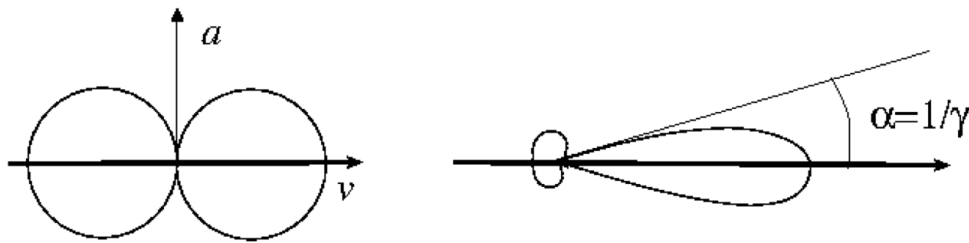
**A universal mechanism** which does not suffer from the problem of discharge is *shock acceleration*.

# **Particle interaction / radiation mechanisms**

## **... electrons**

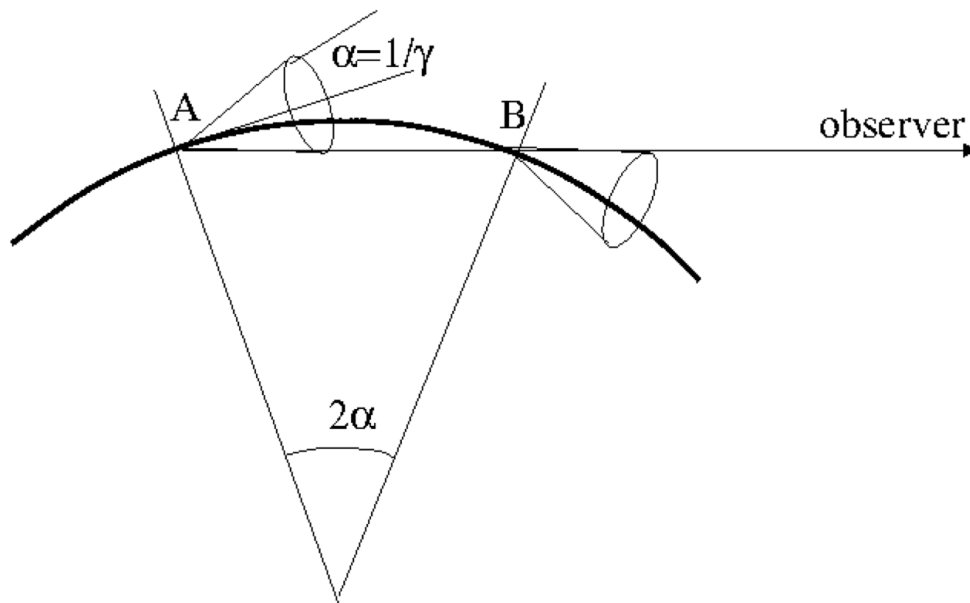
# Basic formula: radiation by accelerated charge

## Curvature radiation



Larmor formula:

$$I = \frac{2\ddot{d}^2}{3} = \frac{2}{3}e^2\gamma^6 \left( a_{\parallel}^2 + \frac{1}{\gamma^2}a_{\perp}^2 \right)$$



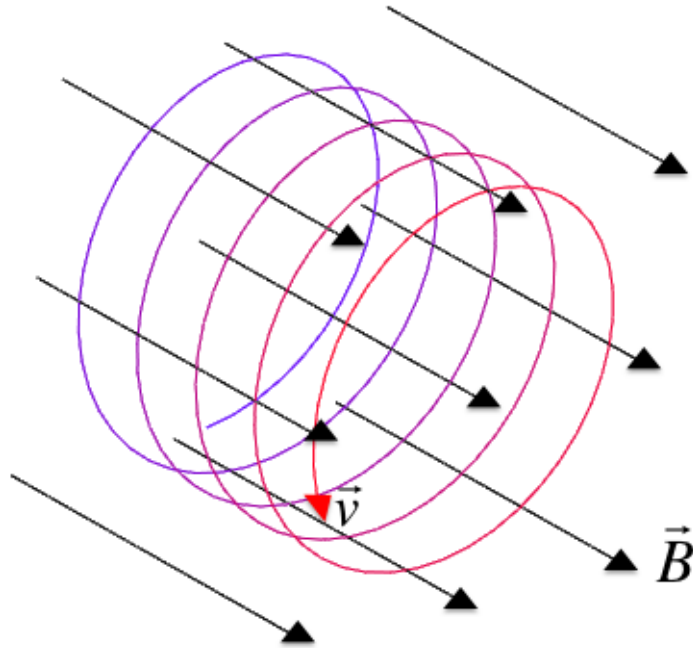
applied to particle moving over a circular orbit:

$$I = \frac{2}{3} \frac{e^2 \gamma^4 v^4}{R^2}$$

Spectrum is peaking at a frequency

$$\omega = \gamma^3 \omega_0 = \frac{\gamma^3 v}{R}$$

# Synchrotron radiation



Larmor formula applied to particle moving over a circular orbit of the radius  $R_L = E / eB$  in magnetic field

$$I = \frac{2}{3} \frac{e^4 B^2 E^2}{m^4}$$

Particle **cooling time**

$$t_{synch} = \frac{E}{dE/dt} = \frac{E}{I} = \frac{3}{2} \frac{m^4}{e^4 B^2 E}$$

$$\simeq 10^4 \frac{m_e^4}{m^4} \left[ \frac{B}{1 \text{ G}} \right]^{-2} \left[ \frac{E_e}{10^{10} \text{ eV}} \right]^{-1} \text{ s}$$

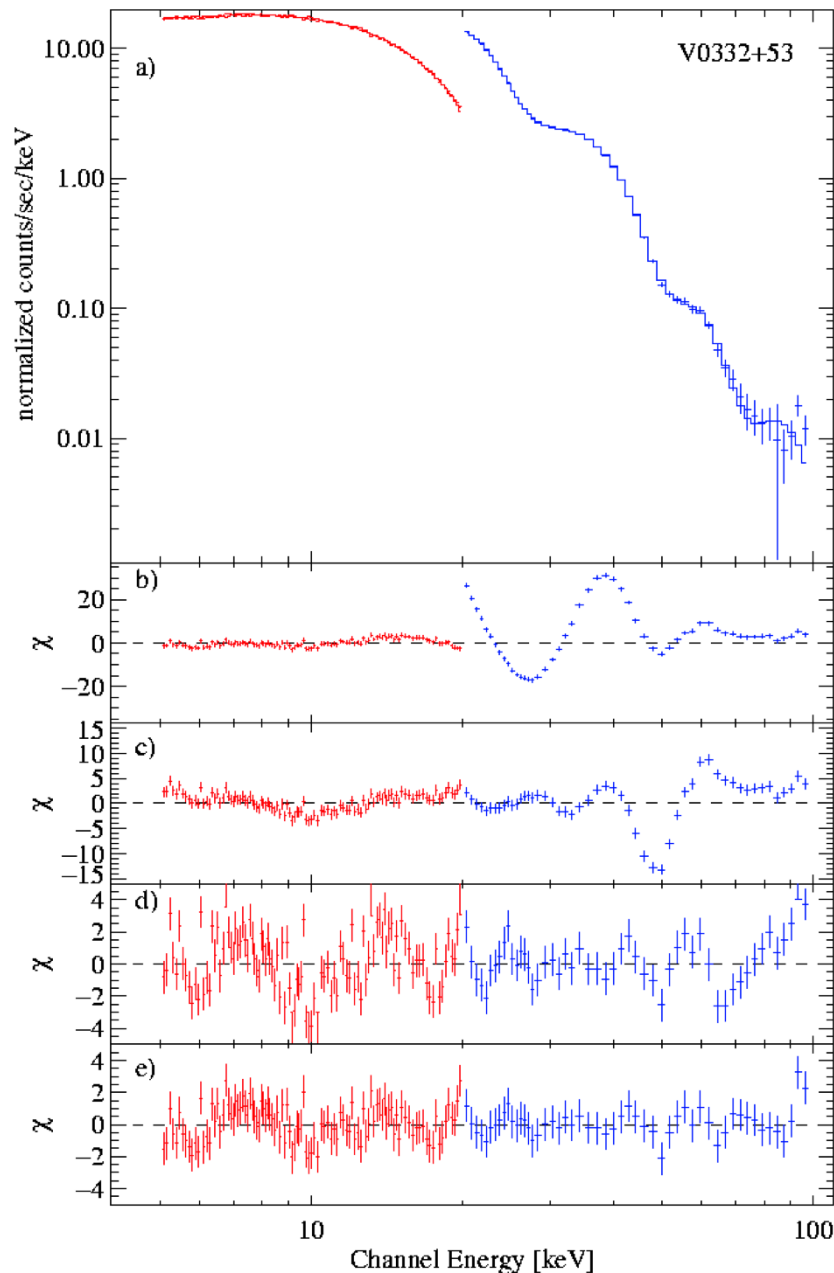
Frequency of gyration for a mildly relativistic electron

$$\omega_B = \frac{m_e}{eB} \simeq 2 \times 10^{-8} \left[ \frac{B}{1 \text{ G}} \right] \text{ eV}$$

Spectrum of radiation peaks at a frequency

$$\omega = \gamma^2 \omega_B = \frac{eBE^2}{m_e^3} \simeq 5 \left[ \frac{B}{1 \text{ G}} \right] \left[ \frac{E}{10^{10} \text{ eV}} \right]^2 \text{ eV}$$

# Cyclotron emission/absorption “lines”



Gyrofrequency reaches the X-ray band if the magnetic field is of the order of  $10^{12}$  G

$$\omega_B = \frac{m_e}{eB} \simeq 20 \left[ \frac{B}{10^{12} \text{ G}} \right] \text{ keV}$$

The gyroradius of non-relativistic electrons in such magnetic field

$$R_L = \frac{m_e}{eB} \simeq 10^{-9} \left[ \frac{B}{10^{12} \text{ cm}} \right]^{-1} \text{ cm}$$

Is comparable to the de Broglie wavelength, so that particle motion is quantized. Electrons are occupying discrete Landau levels  $E_n = \hbar \omega_B (n + 1/2)$  and spectrum of emission / absorption produced by electrons in such magnetic field is (almost) discrete.

Cyclotron emission / absorption lines are observed in X-ray binaries with neutron stars.



# Synchrotron emission from electrons in interstellar medium



Typical magnetic fields in the interstellar media of galaxies are  $B \sim 10 \mu\text{G}$ .

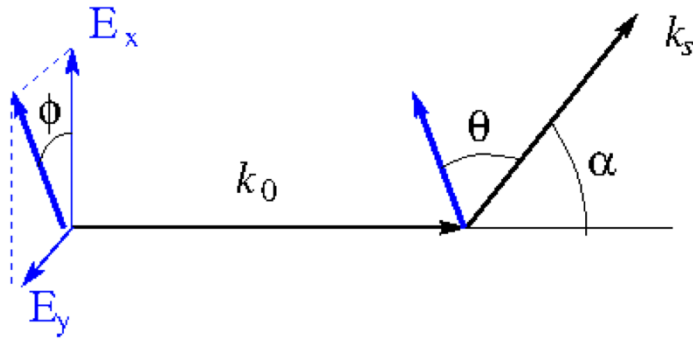
$$\omega \simeq 5 \times 10^{-5} \left[ \frac{B}{10^{-5} \text{ G}} \right] \left[ \frac{E}{10^{10} \text{ eV}} \right]^2 \text{ eV}$$

Electrons producing synchrotron radiation in the radio band have energies in the  $10 \text{ GeV}$  range.

Synchrotron radiation is polarized. Measurements of polarization direction provide information on the structure of magnetic fields in galaxies.



# Compton scattering



Larmor formula applied to the motion of non-relativistic particle in electromagnetic field of isotropic light waves with electric field amplitude  $\mathcal{E}_0$

$$\frac{dE}{dt} \sim e^2 \bar{a}^2 \sim \frac{e^4 \mathcal{E}_0^2}{m^2} = \frac{4}{3} \sigma_T U_{rad}$$

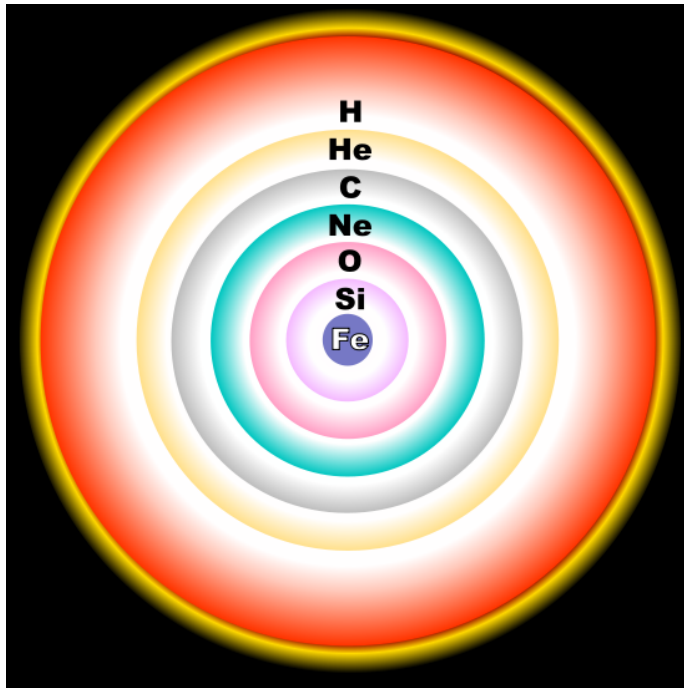
where  $\sigma_T = 6.6 \times 10^{-25} \text{ cm}^2$  is Thomson cross-section and  $U_{rad}$  is the energy density of radiation.

Kinematics of photon-electron collision gives a relation between the energy of incident and outgoing photons  $\epsilon_i, \epsilon_f$ :

$$\epsilon_f = \frac{\epsilon_i}{1 + \frac{\epsilon_i}{m_e} (1 - \cos \theta)}$$

If the energy of incident photons is  $\epsilon_i \ll m_e$ , the energy of outgoing photon is almost equal to the energy of the infalling photon. This regime of Compton scattering is called Thomson scattering.

# Compton scattering in stars



Compton scattering is responsible for the observed properties of stars.

Photons produced by the nucleosynthesis deep inside the star have initially energies in the MeV range.

The MeV gamma-rays do not escape from the interior and instead start to scatter inside the star with the mean free path

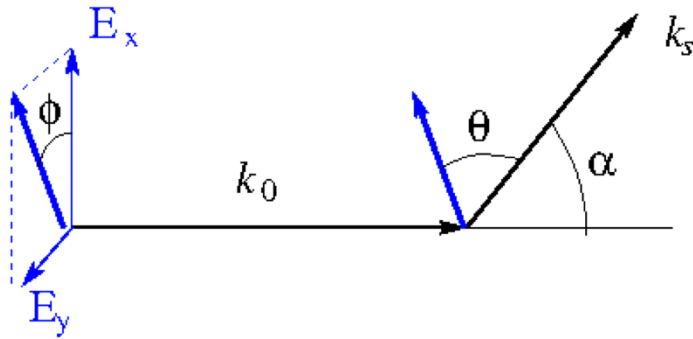
$$\lambda = (\sigma_T n_*)^{-1} \simeq 1 \left[ \frac{n}{10^{24} \text{ cm}^{-3}} \right]^{-1} \text{ cm}$$

The mean free path is much shorter than the size of the star and it takes photon some

$$t \simeq \frac{R_*^2}{\lambda} \simeq 10^4 \left[ \frac{R_*}{10^{11} \text{ cm}} \right]^2 \text{ yr}$$

To get to the stellar surface. Multiple collisions during diffusive propagation of photon toward the star surface lead to thermalization of the photon-plasma system.

# Inverse Compton scattering



Larmor formula applied to the motion of particle in electromagnetic field of isotropic light waves with electric field amplitude  $\mathcal{E}_0$

$$\frac{dE}{dt} \sim \frac{e^4 \mathcal{E}_0^2}{m^2} \gamma^2 v^2 = \frac{4}{3} \sigma_T U_{rad} \gamma^2 v^2$$

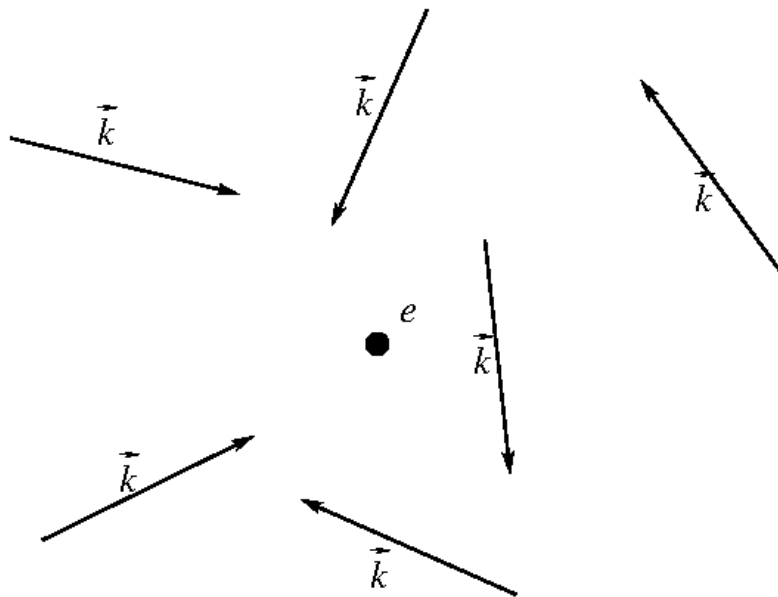
Inverse Compton cooling time for electrons is

$$t_{IC} = \frac{E}{dE/dt} = \frac{3}{4} \frac{m^2}{\sigma_T U_{rad} E}$$

$$\simeq 3 \times 10^7 \left[ \frac{U_{rad}}{1 \text{ eV/cm}^3} \right]^{-1} \left[ \frac{E_e}{10^{10} \text{ eV}} \right]^{-1} \text{ s}$$

Spectrum of radiation peaks at a frequency

$$\omega = \gamma^2 \omega_0 \simeq 0.5 \left[ \frac{\omega_0}{1 \text{ eV}} \right] \left[ \frac{E}{10^{10} \text{ eV}} \right]^2 \text{ GeV}$$



# Synchrotron vs. inverse Compton

Energy loss rate of electron scales with the square of electron energy and is proportional to the energy density of magnetic field

$$I = \frac{2}{3} \frac{e^4 B^2 E^2}{m^4} = \frac{4}{3} \sigma_T U_B \gamma^2$$

Electron cooling time scale is inversely proportional to electron energy

$$t_{synch} \simeq 10^4 \left[ \frac{B}{1 \text{ G}} \right]^{-2} \left[ \frac{E_e}{10^{10} \text{ eV}} \right]^{-1} \text{ s}$$

Typical energy of inverse Compton photons scales with the square of electron energy

$$\omega \simeq 5 \left[ \frac{B}{1 \text{ G}} \right] \left[ \frac{E}{10^{10} \text{ eV}} \right]^2 \text{ eV}$$

Energy loss rate of electron scales with the square of electron energy and is proportional to the energy density of radiation

$$\frac{dE}{dt} \simeq \frac{4}{3} \sigma_T U_{rad} \gamma^2$$

Electron cooling time scales inversely proportional to electron energy

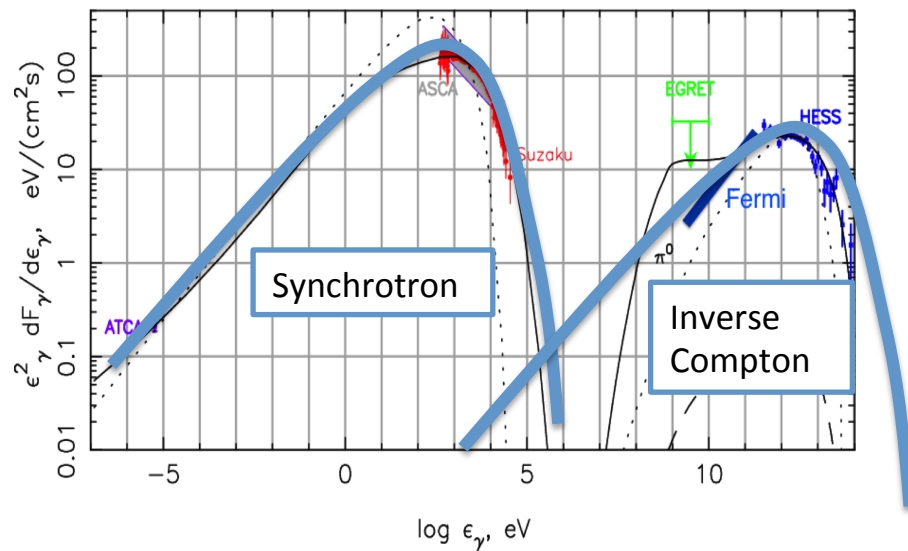
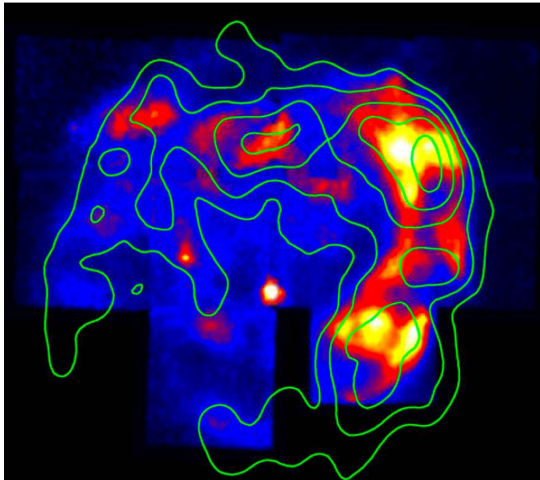
$$t_{IC} \simeq 3 \times 10^7 \left[ \frac{U_{rad}}{1 \text{ eV/cm}^3} \right]^{-1} \left[ \frac{E_e}{10^{10} \text{ eV}} \right]^{-1} \text{ s}$$

Typical energy of inverse Compton photons scales with the square of electron energy

$$\omega \simeq 0.5 \left[ \frac{\omega_0}{1 \text{ eV}} \right] \left[ \frac{E}{10^{10} \text{ eV}} \right]^2 \text{ GeV}$$

Ratio of synchrotron to inverse Compton luminosity of an astronomical source is  
Equal to the ratio of the energy densities of magnetic field and radiation  $U_B / U_{rad}$

# Synchrotron – inverse Compton emission



A combination of synchrotron and inverse Compton emission is a typical spectral appearance of high-energy sources.

Example: RX J1713 supernova remnant:

$$U_B \approx 10U_{\text{rad}} \sim 10 - 30 \text{ eV/cm}^3; \quad B \approx 10 \mu\text{G}.$$

( $U_{\text{rad}}$  is the energy density of interstellar radiation field).

$$\omega \approx 0.5 \left[ \frac{B}{10^{-5} \text{ G}} \right] \left[ \frac{E}{3 \times 10^{13} \text{ eV}} \right]^2 \text{ keV}$$

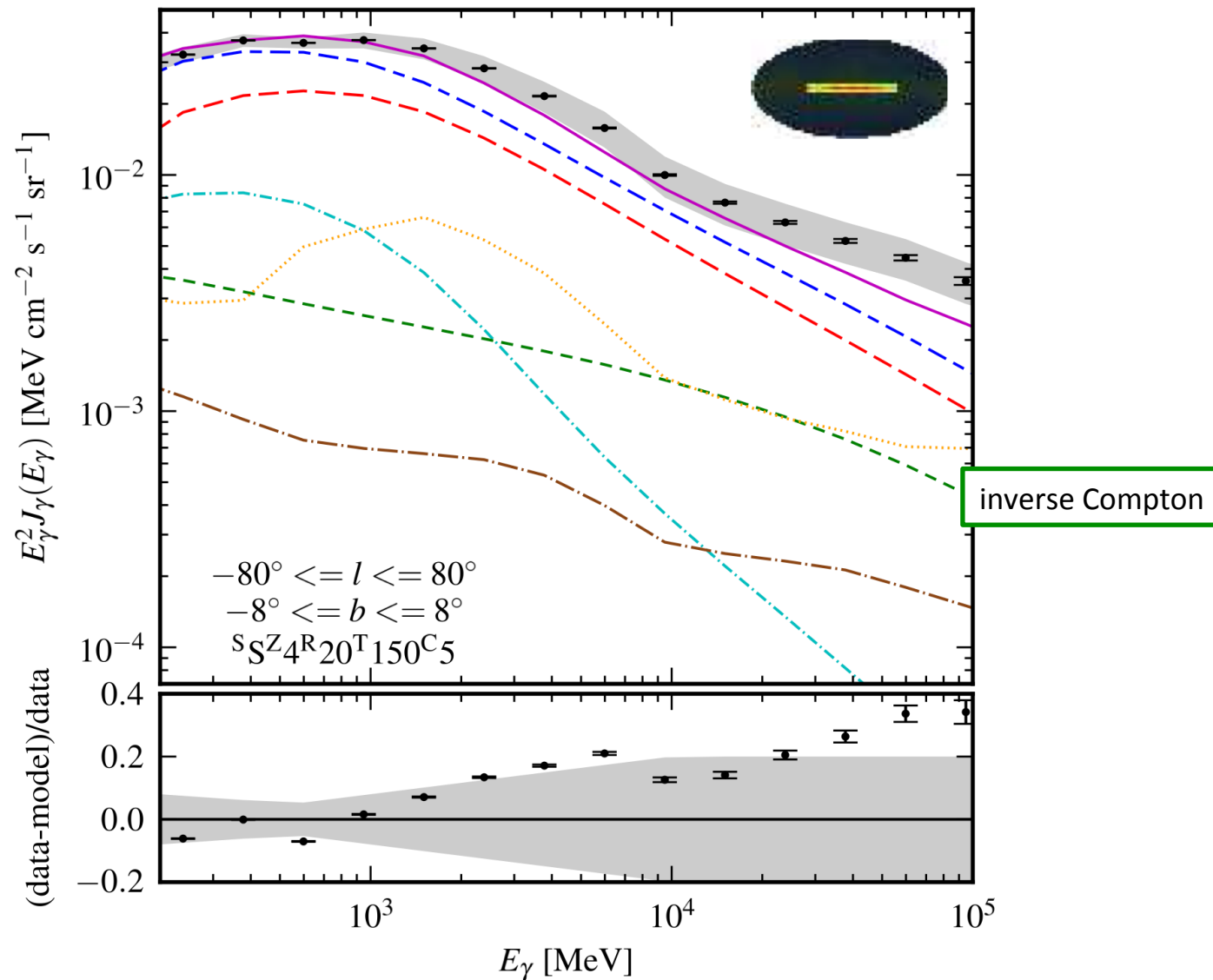
Energies of electrons retained in the remnant reach 30 TeV.

Comparing this estimate with the “Hillas plot” estimate

$$E_{\text{max}} \approx 3 \times 10^{15} \left[ \frac{B}{10^{-5} \text{ G}} \right] \left[ \frac{R}{10^{18} \text{ cm}} \right] \text{ eV}$$

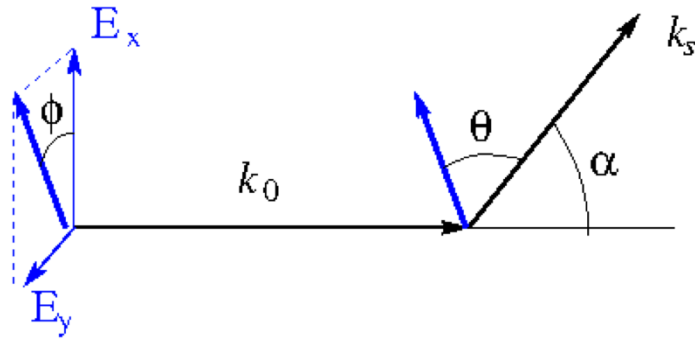
one finds that the supernova remnant “underperforms” as particle accelerator machine.

# Inverse Compton scattering by cosmic ray electrons



Spectrum of diffuse gamma-ray emission from the inner Galaxy

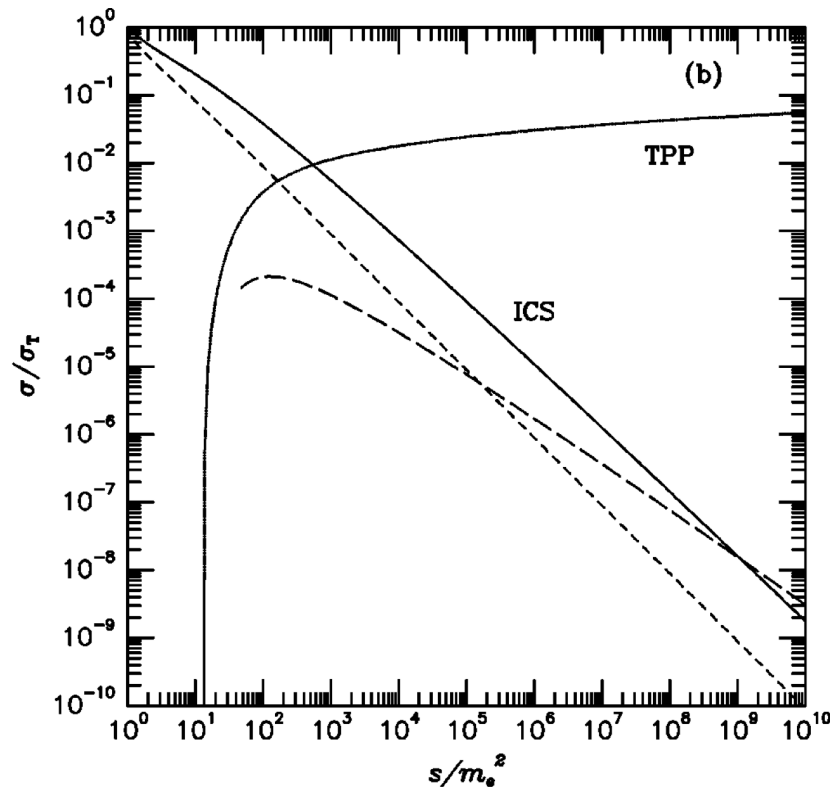
# Inverse Compton scattering in Klein-Nishina regime



$$\omega = \gamma^2 \omega_0 \simeq 0.5 \left[ \frac{\omega_0}{1 \text{ eV}} \right] \left[ \frac{E}{10^{10} \text{ eV}} \right]^2 \text{ GeV}$$

The energy of upscattered photons becomes comparable to the energy of electrons as soon as  $E_e \omega_0 \simeq m_e^2$ . Starting from this energy, the inverse Compton scattering regime changes and each scattering takes away significant fraction of electron energy, so that  $\omega \simeq E$  holds.

This regime is called Klein-Nishina regime of inverse Compton scattering.

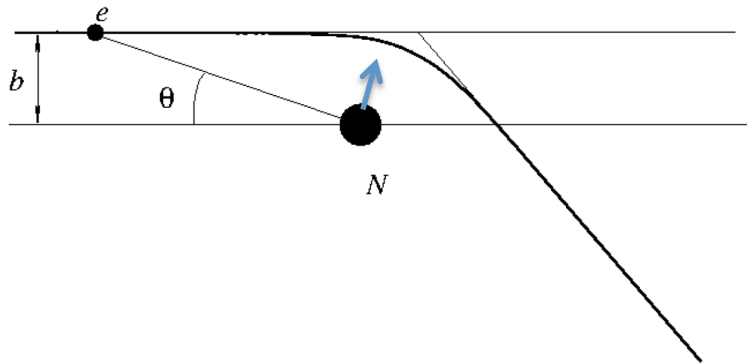


The cross-section of inverse Compton scattering in Klein-Nishina regime drops with the increase of  $s = \omega_0 E$  so that the inverse Compton cooling time

$$t_{IC} \sim \frac{1}{\sigma_{KN} n_{ph}}$$

increases.

# Bremsstrahlung and Coulomb loss



Larmor formula applied to the motion of particle deflected by electric fields of atomic nuclei of charge  $Z$  in a gas of density  $n$  (up to a logarithmic factor)

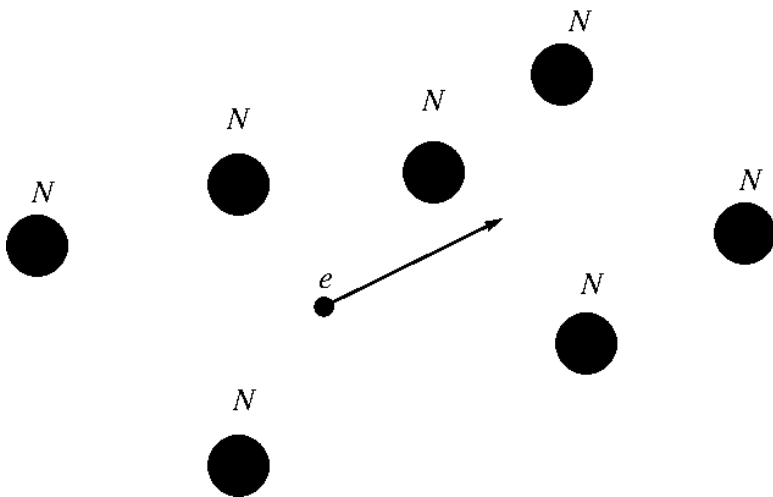
$$\frac{dE}{dt} \approx 10 \frac{Z^2 e^6 n E}{m_e^2}$$

**Bremsstrahlung** cooling time for electrons is

$$t_{Brems} = \frac{E}{dE/dt} = \frac{m_e^2}{10 Z^2 e^6 n} \approx 4 \times 10^7 \left[ \frac{n}{1 \text{ cm}^{-3}} \right]^{-1} \text{ yr}$$

Spectrum of radiation peaks at a frequency

$$\omega \approx E$$



Interactions with atomic nuclei result also in non-radiative **Coulomb loss** (on nuclear recoils) with the energy loss rate (Bethe-Bloch formula)

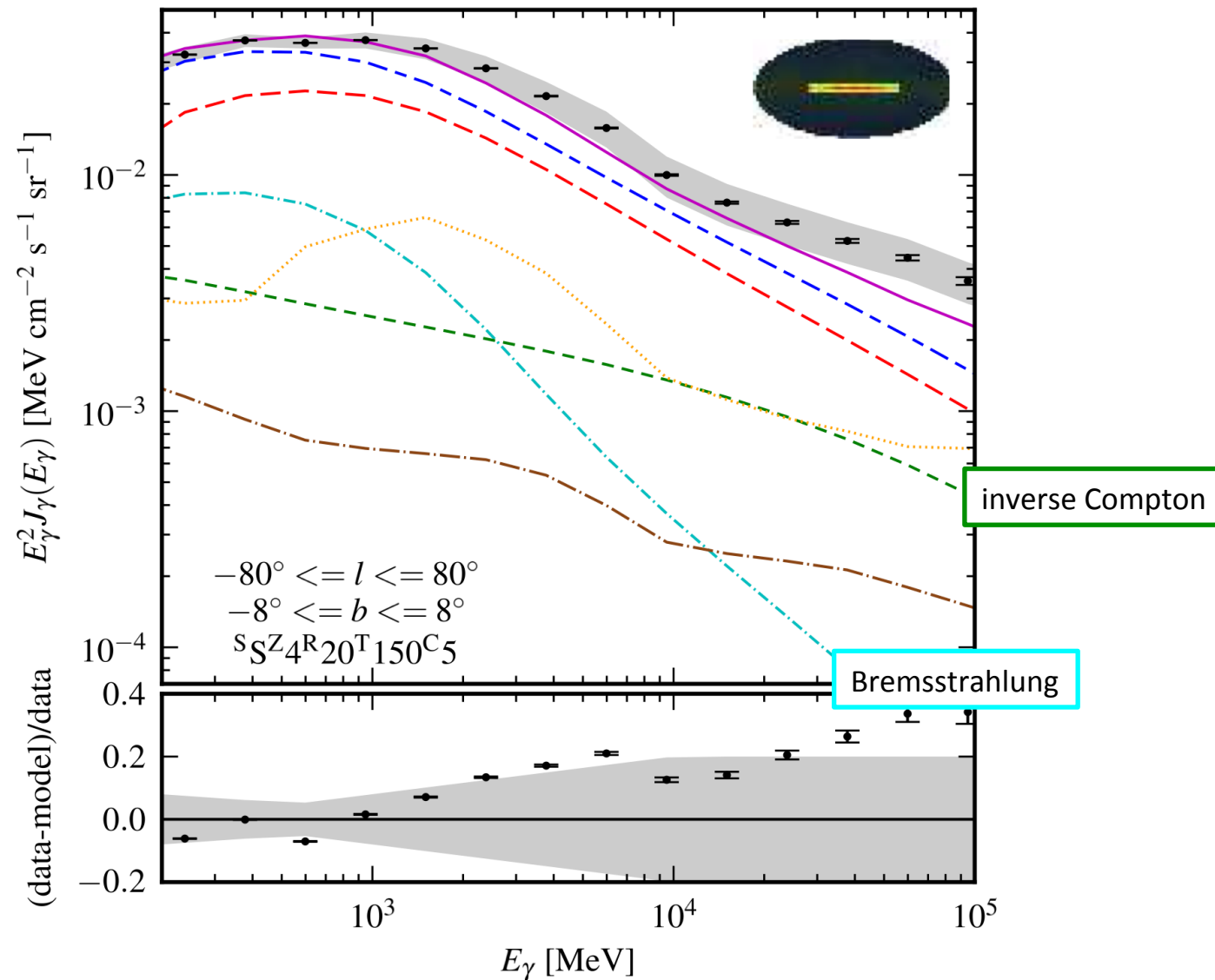
$$\frac{dE}{dt} \approx \frac{4\pi Z^2 e^4 n}{m_e v^2} \left[ \ln \left( \frac{2\gamma^2 m v^2}{I} \right) - v^2 \right]$$

With the Coulomb cooling time

$$t_{Coul} \approx e^2 \gamma t_{Brems}$$

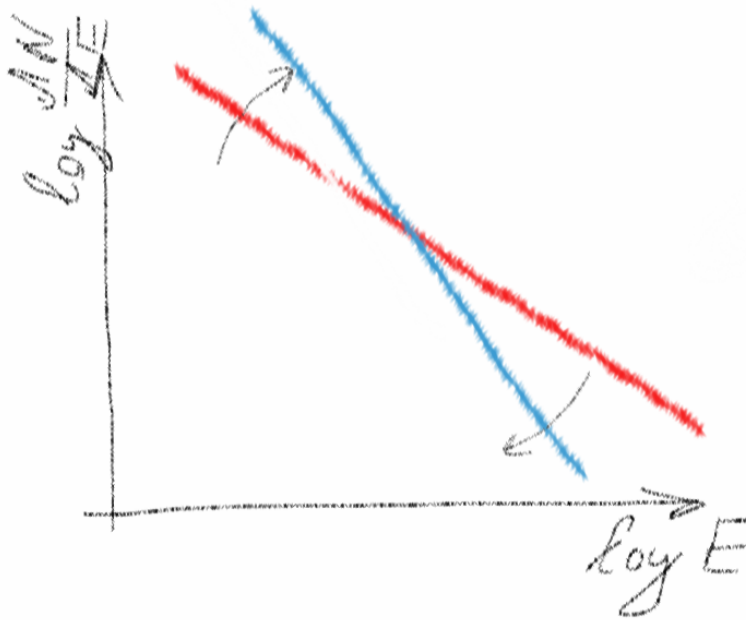


# Pion production in proton-proton collisions



Spectrum of diffuse gamma-ray emission from the inner Galaxy

# Effects of radiative and Coulomb cooling



Acceleration process injects particles with certain energy distribution  $dN / dE = Q(E)$ . This distribution is modified by the cooling processes. Evolution of the distribution is described as motion in the energy space

$$\frac{\partial f}{\partial t} + \frac{\partial}{\partial E}(\dot{E}f(E)) = Q(E,t) - \frac{f}{\tau_{esc}}$$

In the absence of escape the kinetic equation has a steady state solution

$$f(E) = \frac{1}{\dot{E}} \int_E^\infty dE' Q(E')$$

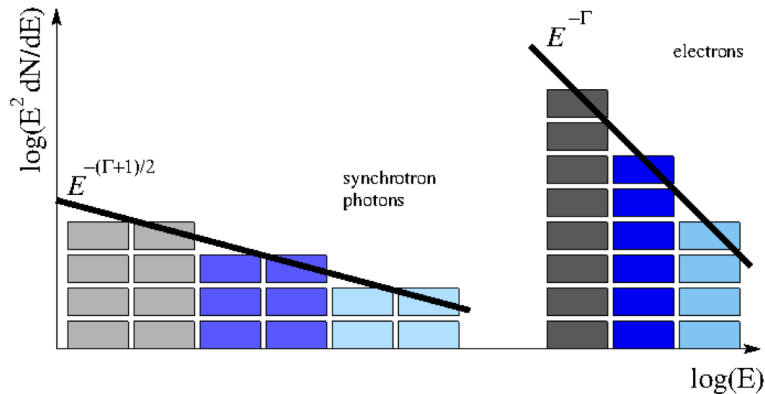
Example: effect of synchrotron and inverse Compton cooling on power-law particle injection spectrum

$$Q(E) \sim E^{-p}$$

$$f(E) \sim \frac{1}{E^2} \int_E^\infty dE' E'^{-p} \sim E^{-(p+1)}$$

By the same argument one finds that Bremsstrahlung energy loss does not affect the slope of particle spectrum. Coulomb loss hardens it.

# Radiation from a distribution of particles



Acceleration and cooling processes form broad energy distributions of particles  $dN / dE = f(E)$ . Radiation from a broad band particle distribution has a broad band spectrum

$$\phi(E_\gamma) = \int \frac{dN}{dE_e} \Phi(E_e, E_\gamma) dE_e$$

where  $\Phi(E_e, E_\gamma)$  is the spectrum of emission from a monoenergetic electrons with energy  $E_e$ .

Example: spectrum of synchrotron emission from a powerlaw distribution of electrons,  $dN / dE \sim E^{-p}$ . In a rough “delta-function” approximation,

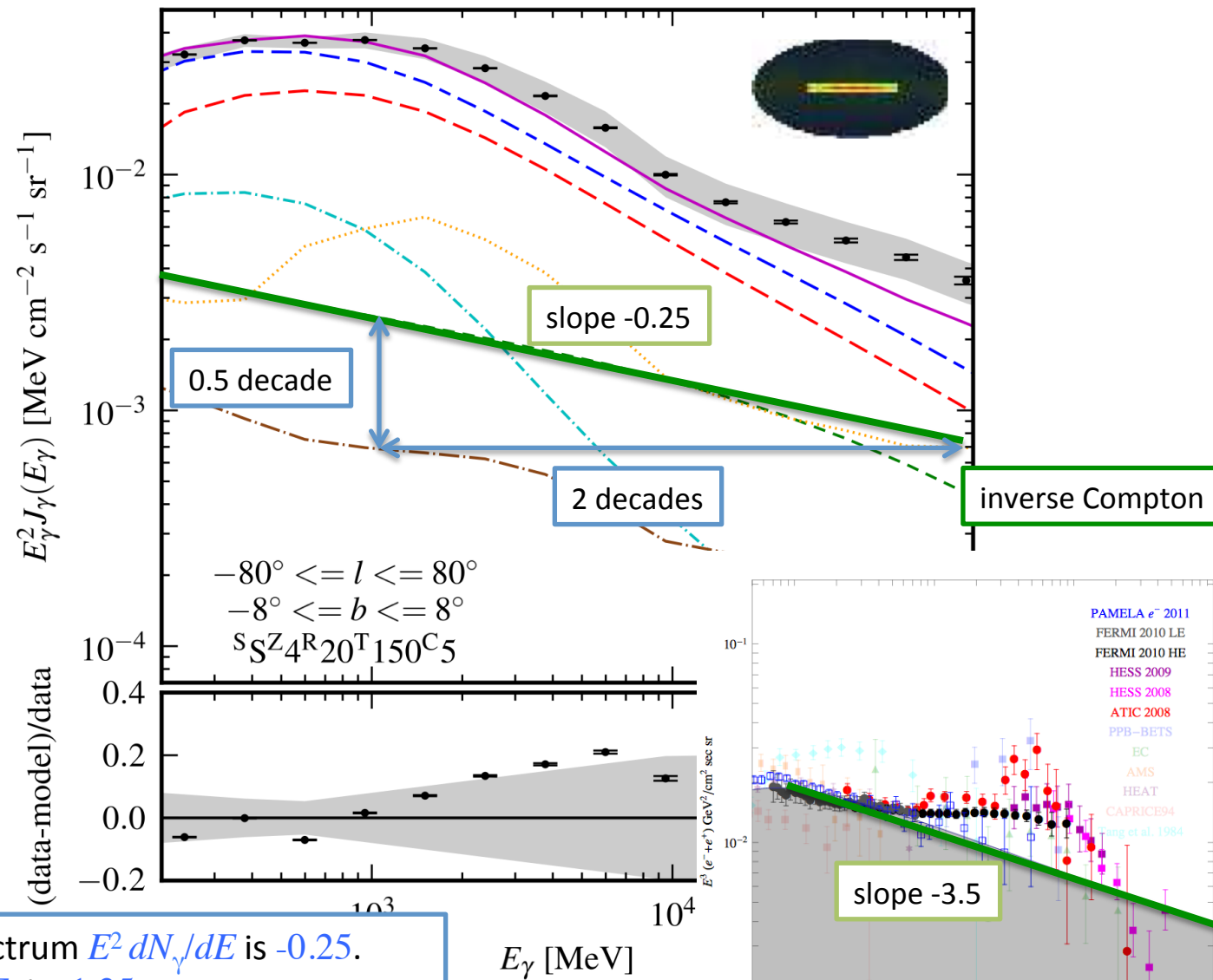
$$\begin{aligned} \Phi(E_e, E_\gamma) &\simeq I_{\text{synch}}(E_e) \delta(E - \omega_{\text{synch}}) \\ &\sim \frac{e^4 B^2 E_e^2}{m_e^4} \delta\left(E_\gamma - \frac{e B E_e^2}{m_e^3}\right) \end{aligned}$$

so that

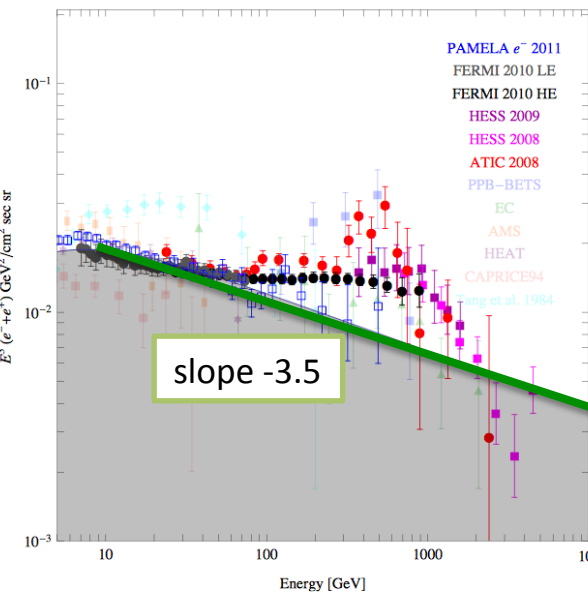
$$\phi(E_\gamma) \sim \int E_e^{2-p} \delta\left(E_\gamma - \frac{e B E_e^2}{m_e^3}\right) dE_e \sim E_\gamma^{(1-p)/2}$$

The same relation between  $p$  and the slope of the photon spectrum holds for Inverse Compton.

# Pion production in proton-proton collisions



Slope of the spectrum  $E^2 dN_\gamma/dE$  is -0.25.  
 Slope of  $EdN_\gamma/dE$  is -1.25.  
 Assumed slope of electron spectrum is  $p=3.5$



**Particle interaction / radiation mechanisms**  
**... protons and atomic nuclei**

# Energy losses of protons and atomic nuclei

## Electromagnetic processes

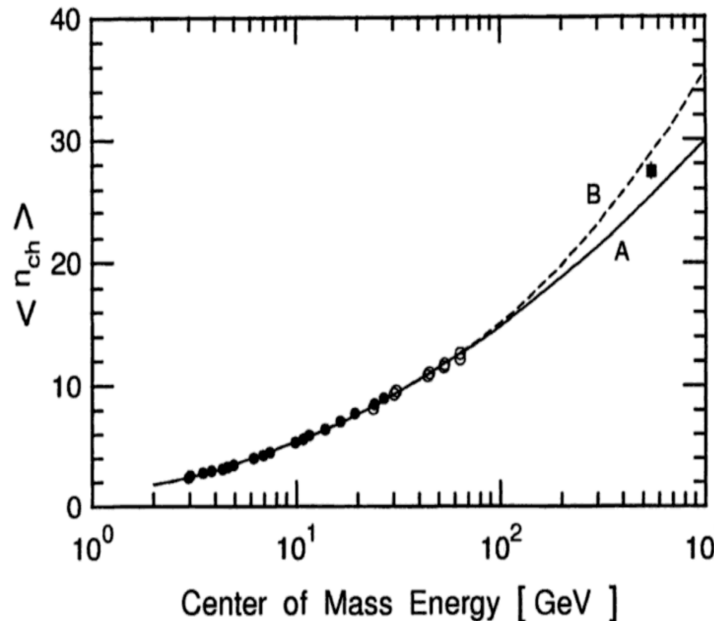
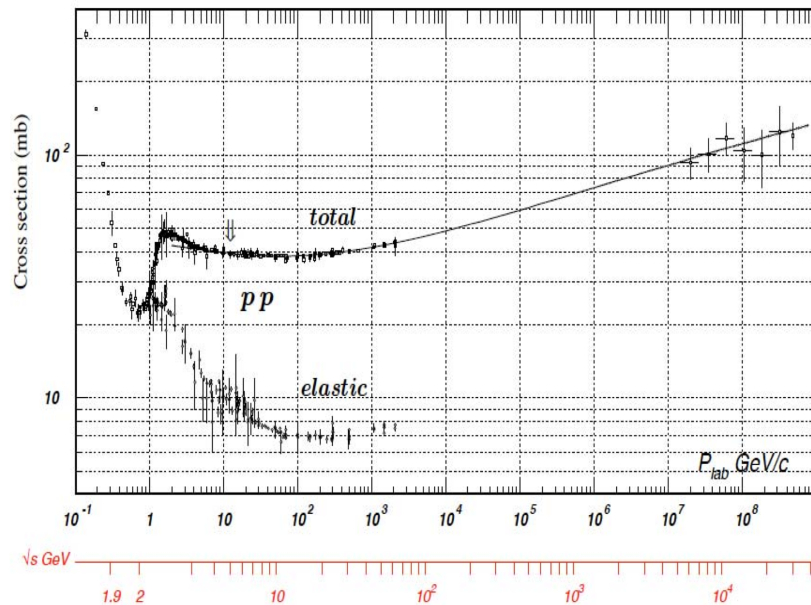
$$t_{\text{synch}} = \frac{E_e}{dE_e/dt} = \frac{3m_e^4}{2e^4 E_e B^2} \text{ (synchrotron)} \rightarrow = \frac{3m_p^4}{2e^4 E_p B^2} \approx 10^{10} \left[ \frac{B}{1 \text{ G}} \right]^{-2} \left[ \frac{E_p}{10^{10} \text{ eV}} \right]^{-1} \text{ yr}$$

$$t_{\text{IC}} = \frac{3m_e^2}{4\sigma_T U_{\text{rad}} E_e} \text{ (inv. Compton)} \Rightarrow = \frac{9m_p^4}{32\pi e^2 U_{\text{rad}} E_p} \approx 10^{21} \left[ \frac{E_p}{10^{10} \text{ eV}} \right]^{-1} \left[ \frac{U_{\text{rad}}}{1 \text{ eV/cm}^3} \right]^{-1} \text{ yr}$$

$$t_{\text{Brems}} \approx \frac{m_e^2}{16 Z(Z+1) e^6 n} \text{ (Bremsstrahlung)} \rightarrow \approx \frac{m_p}{m_e} \frac{m_e^2}{16 e^6 n} \approx 4 \times 10^{10} \left[ \frac{n}{1 \text{ cm}^{-3}} \right]^{-1} \text{ yr}$$

The rate of electromagnetic processes for protons is suppressed by powers of  $(m_e/m_p)$  and these losses are much less important for the CR nuclei than for electrons and positrons.

# Pion production in proton-proton collisions



Main energy loss channels for high-energy protons and atomic nuclei are via inelastic collisions with ambient protons / nuclei and with photons.

Example: inelastic collisions resulting in production of pions  $p + N \rightarrow p(n) + \tilde{N} + \pi^{0,\pm}$ . Such interaction channels are possible above certain energy threshold

$$E_1 - m_p > E_{thr,\pi} = \frac{m_\pi^2 + 4m_\pi m_p}{2m_p} = 0.28 \text{ GeV}$$

Cross-section of pion production interactions in  $pp$  collisions grows logarithmically with energy starting from the value  $\sigma_{pp} \simeq 4 \times 10^{-26} \text{ cm}^2$  close to the threshold.

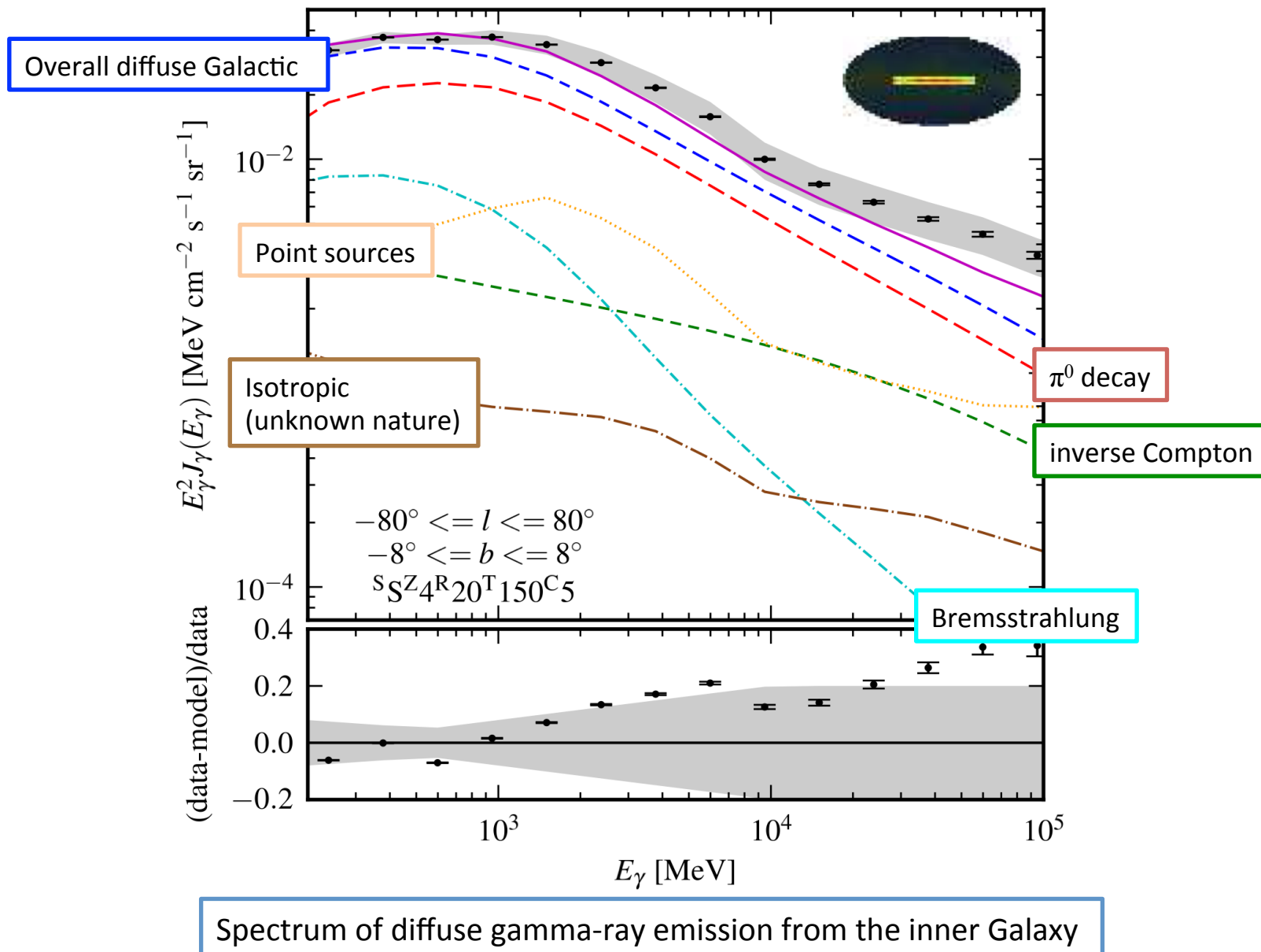
Pion production energy loss time is

$$t_{pp} = \frac{1}{\kappa \sigma_{pp} n} \simeq 10^8 \left[ \frac{n}{1 \text{ cm}^{-3}} \right]^{-1} \text{ yr}$$

where  $\kappa \sim 0.2 \dots 0.5$  is typical inelasticity of collisions (fractional energy loss of high-energy proton in one collision).

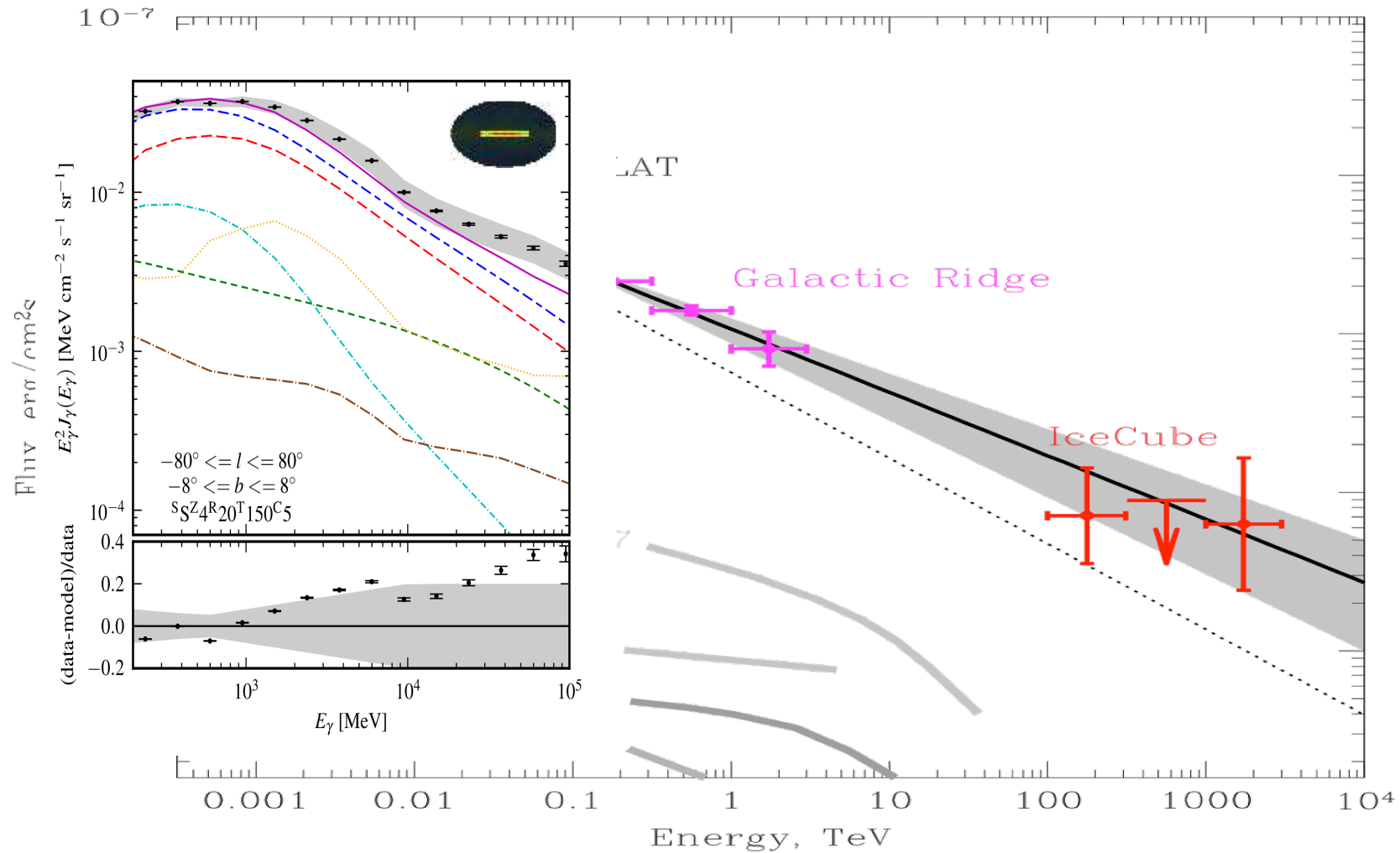
Pion production results in comparable fluxes of gamma-rays and neutrinos.

# Pion production in proton-proton collisions



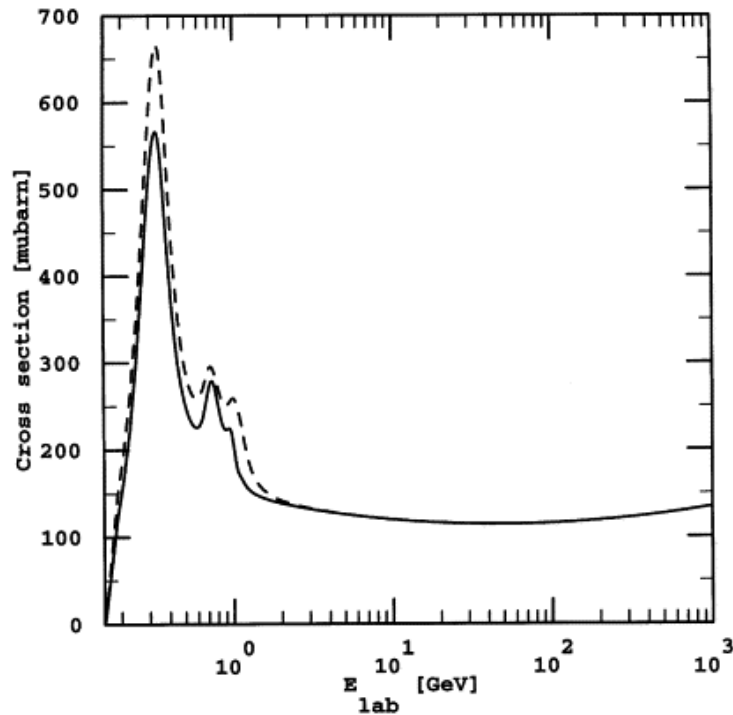


# Pion production in proton-proton collisions



Neutrino signal from the direction of the Galactic Ridge

# Pion production in proton-photon collisions



The threshold of pion production in proton-photon collisions is

$$E_p > \frac{m_\pi + 2m_p m_\pi}{4\epsilon_{ph}} \simeq 10^{17} \left[ \frac{\epsilon_{ph}}{1 \text{ eV}} \right]^{-1} \text{ eV}$$

The collision cross-section is

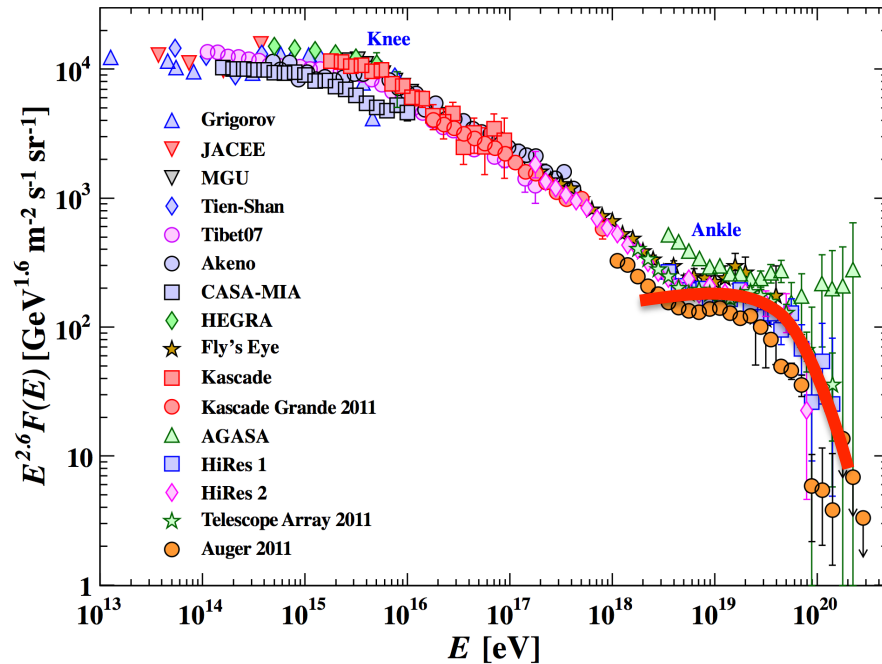
$$\sigma_{p\gamma} \simeq (1..6) \times 10^{-28} \text{ cm}^2$$

The energy loss time due to the photo-pion production is

$$t_{p\gamma} = \frac{1}{\kappa \sigma_{p\gamma} n_{ph}} \simeq 7 \times 10^9 \left[ \frac{n_{ph}}{1 \text{ cm}^{-3}} \right]^{-1} \text{ yr}$$

where  $\kappa \approx 0.2$  is inelasticity of the  $p\gamma$  collisions.

# Pion production in proton-photon collisions



Ultra-High-Energy CRs (UHECR) with energies in excess of the threshold of pion production on CMB

$$E_p > \frac{m_\pi + 2m_p m_\pi}{4\epsilon_{ph}} \simeq 10^{20} \left[ \frac{\epsilon_{ph}}{10^{-3} \text{ eV}} \right]^{-1} \text{ eV}$$

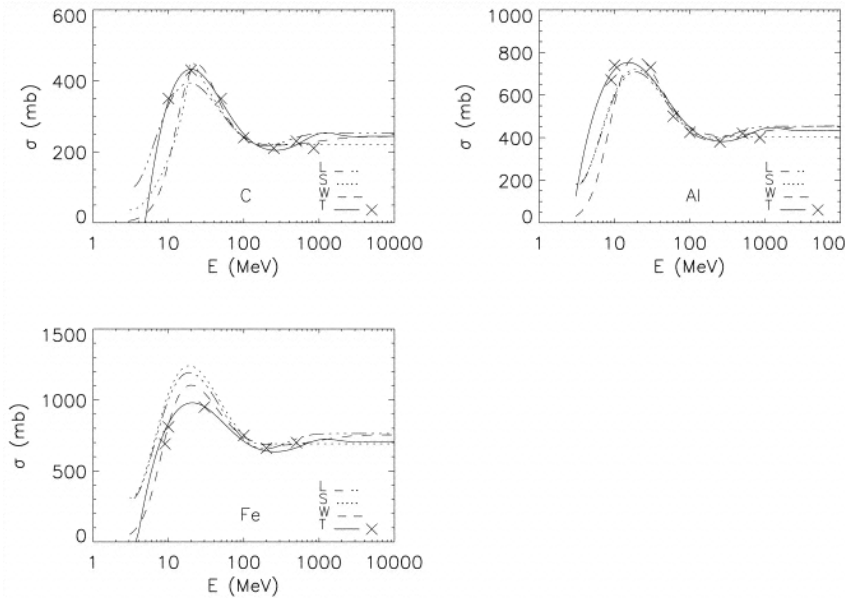
lose their energy on the pion production within the distance range

$$d_{p\gamma} = \frac{1}{\kappa \sigma_{p\gamma} n_{ph}} \simeq 10 \left[ \frac{n_{ph}}{400 \text{ cm}^{-3}} \right]^{-1} \text{ Mpc}$$

Pion production energy loss of UHECR should suppress the flux of CRs from distant sources.

This effect is known under the name GZK effect for Greisen-Zatsepin-Kuzmin.

# Spallation in nuclei collisions



Main inelastic collision channel of atomic nuclei is the break up onto smaller nuclei (preferentially via stripping-off single nucleons or  $\alpha$ -particles).

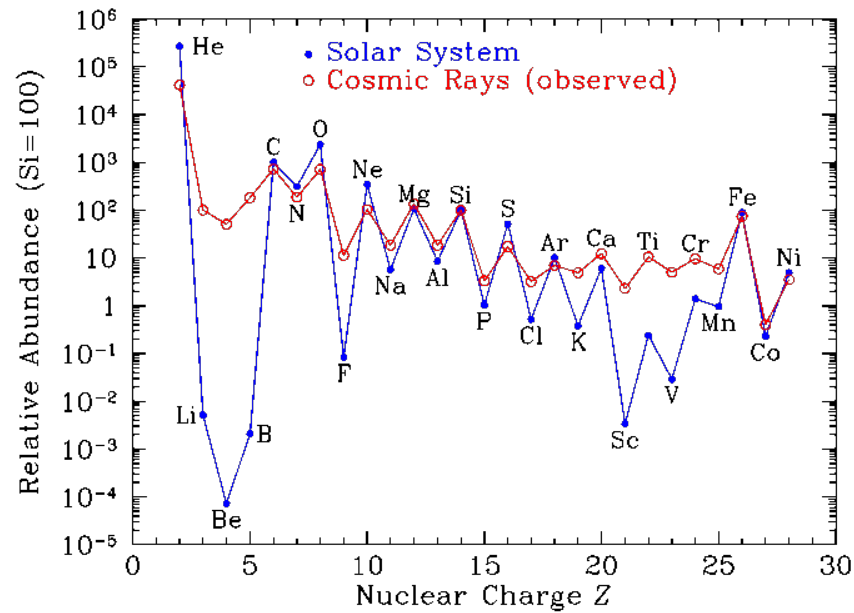
The process sets on as soon as the energy transfer in collisions is larger than **1-10 MeV**. The cross-section of the process is close to the geometrical cross-section of the nucleus

$$\sigma_{sp} \simeq 4\pi A^{2/3} r_p^2 \simeq 2 \times 10^{-25} A^{2/3} \text{ cm}^2$$

Nuclei are disintegrated on the time scale

$$t_{sp} = \frac{1}{\sigma_{sp} n} \simeq 5 \times 10^6 A^{-2/3} \left[ \frac{n}{1 \text{ cm}^{-3}} \right]^{-1} \text{ yr}$$

# Spallation in collisions of cosmic ray nuclei



Certain elements (like e.g. B) are not produced abundantly in stellar nucleosynthesis. However, they are more abundant in cosmic rays. This is explained by production via spallation of heavier nuclei (e.g. C):

$$\dot{n}_B = -\frac{n_B}{t_{esc}} + (\sigma_{sp,C} v n) n_C$$

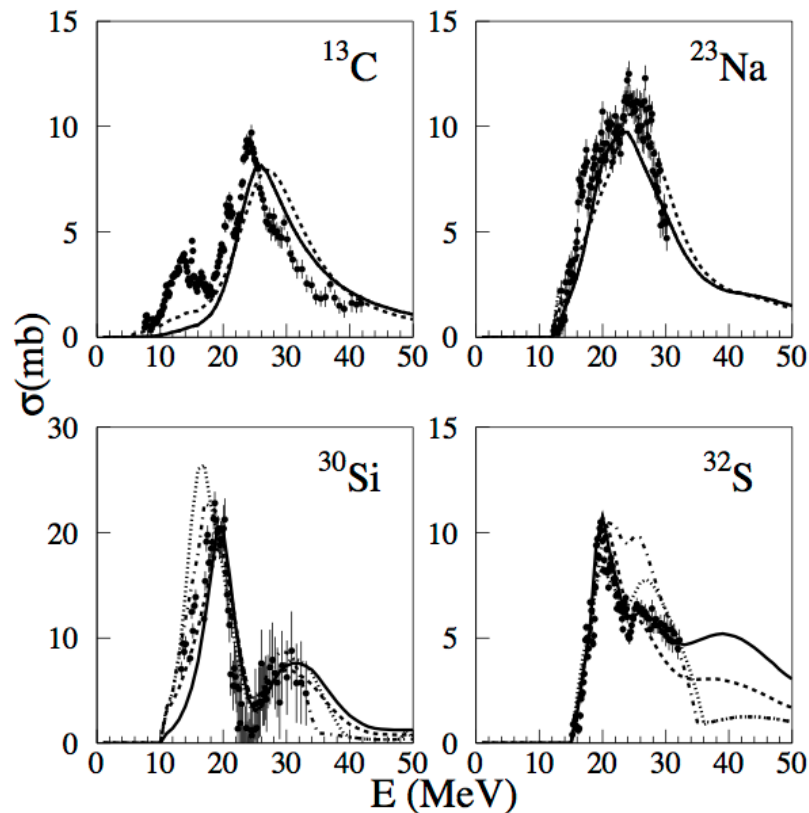
As a result, the steady-state B/C ratio is

$$\frac{n_B}{n_C} = \sigma_{sp,C} v n t_{esc}$$

Knowing the spallation cross-section and measuring B/C ratio in the cosmic ray flux one gets an estimate of the escape time of cosmic rays from the Galactic Disk

$$t_{esc} \sim 10^7 \text{ yr.}$$

# Photo-disintegration in nuclei – photon collisions



High-energy nuclei could also be destroyed in interactions with low energy photons.

The process sets on as soon as the energy transfer in collisions is larger than **1-10 MeV**. Energy of soft photon in the reference frame of the nucleus is

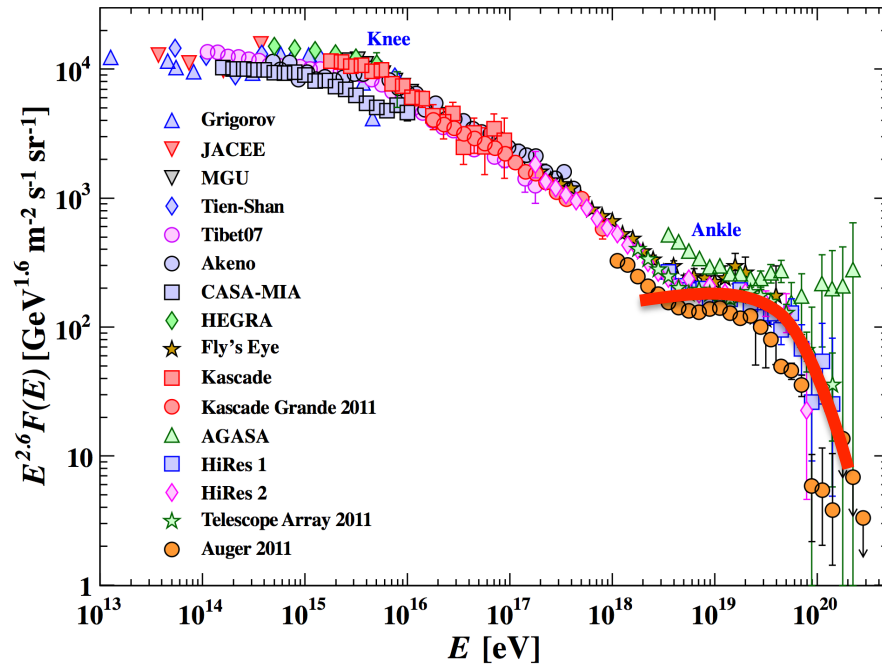
$$\epsilon_{ph'} \sim \left( \frac{E_N}{Am_p} \right) \epsilon_{ph} \approx 10^6 \left[ \frac{A}{56} \right]^{-1} \left[ \frac{E_N}{10^{17} \text{ eV}} \right] \left[ \frac{\epsilon_{ph}}{1 \text{ eV}} \right] \text{ eV}$$

Photons of visible light could destroy atomic nuclei with energies above  $\sim 10^{17}$  eV.

Cross-section of the photo-disintegration is in the range  $\sigma_{N\gamma} \approx 10^{-26} - 10^{-25} \text{ cm}^2$ . Photo-disintegration time is thus

$$t_{N\gamma} = \frac{1}{K \sigma_{N\gamma} n_{ph}} \approx 10^9 \left[ \frac{A}{56} \right]^x \left[ \frac{n_{ph}}{1 \text{ cm}^{-3}} \right]^{-1} \text{ yr}$$

# Photo-disintegration of UHECR nuclei



Atomic nuclei with energies in excess of the threshold of photo-disintegration loose their energy within the distance range

$$d_{N\gamma} = \frac{1}{\kappa \sigma_{N\gamma} n_{ph}} \simeq 1 \left[ \frac{A}{56} \right]^x \left[ \frac{n_{ph}}{400 \text{ cm}^{-3}} \right]^{-1} \text{ Mpc}$$

Iron nuclei with energies in the  $10^{20}$  eV range are mostly disintegrated in interactions with photon from the Wien tail of the CMB spectrum and/or with the far-infrared photons of Extragalactic Background Light.

This leads to suppression for the nuclear UHECR flux, similar to the suppression of the proton UHECR flux due to the GZK effect.

# Summary

Main radiative energy loss channels of high-energy electrons are on [synchrotron](#), [inverse Compton](#) and [Bremsstrahlung](#) emission.

All the three cases are particular examples of dipole radiation. The energy loss formulae are derived from the [Larmor formula](#).

[Synchrotron – inverse Compton](#) emission produces a characteristic two-bump spectrum of high-energy sources. The ratio of the heights of the two bumps is equal to the ratio of the energy densities of magnetic field and radiation in the source.

Main radiative energy loss for high-energy protons and nuclei is via [production and decay of pions](#).

Pion production results in emission of comparable amounts of [gamma-rays](#) and [neutrinos](#).

Pion production occurs in interactions of high-energy protons / nuclei with ambient protons / nuclei and with radiation fields.

High-energy atomic nuclei suffer from non-radiative [spallation](#) and [photo-disintegration](#) energy losses.